

Selective Mott transition and heavy fermions

C. Pépin

SPhT, CEA-Saclay, L'Orme des Merisiers, 91191 Gif-sur-Yvette, France

(Received 19 February 2008; revised manuscript received 23 April 2008; published 23 June 2008)

Starting with an extended version of the Anderson lattice where the f electrons are allowed a weak dispersion, we examine the possibility of a Mott localization of the f electrons for a finite value of the hybridization V . We study the fluctuations at the quantum critical point (QCP) where the f electrons localize. We find that they are in the same universality class as for the Kondo breakdown QCP, with the following notable features. The quantum critical regime sees the appearance of an additional energy scale separating two universality classes. In the low energy regime, the fluctuations are dominated by massless gauge modes, while in the intermediate energy regime, the fluctuations of the modulus of the order parameter are the most relevant ones. In the latter regime, electric transport simplifies drastically, leading to a quasilinear resistivity in three dimensional and anomalous exponents lower than T in two dimensional. This rather unique feature of the quantum critical regime enables us to make experimentally testable predictions.

DOI: [10.1103/PhysRevB.77.245129](https://doi.org/10.1103/PhysRevB.77.245129)

PACS number(s): 71.27.+a, 72.15.Qm, 75.20.Hr, 75.30.Mb

I. INTRODUCTION

Several years of intense experimental studies of quantum criticality in intermetallic and heavy fermion compounds have lead to a growing evidence for a violation of the standard Landau–Fermi liquid theory of the metallic behavior. Experimental phase diagrams use an external tuning parameter, such as the chemical pressure, the hydrostatic pressure, or the magnetic field, to explore phase transitions at a temperature very close to the absolute zero. These phase transitions exhibit a regime of very strong quantum fluctuations—the quantum critical regime—where anomalous thermodynamic and transport exponents are observed. A heavy fermion compound consists in a lattice of “big” atoms, such as Ce, U, or Yb, alloyed with a metal. The magnetic multiplet in the heavy atoms is determined by Hund's rules and spin-orbit interaction. For example, after spin-orbit interaction, the magnetic moment of Ce $4f^1$ ($S=1/2$, $L=3$) is $J=5/2$, for Yb $4f^{13}$ ($S=1/2$, $L=3$) we get $J=7/2$, and for U $5f^2$ ($S=1$, $L=3+2$) it leads to $J=4$. The degeneracy is then split by the lattice crystal field effects, finally leading to a Kramers doublet. The apparent chemical complexity of this material has to be kept in mind for any investigation of their anomalous experimental properties. In particular, the Anderson lattice model, which is standard in describing those compounds, relies upon the assumption that the Kramers doublets are well formed¹ and thus, at low energy, one effectively considers that the physics is thoroughly described by f electrons, sitting on the impurity atoms, subjected to strong Coulomb interactions, and hybridizing with the conduction electrons of the metal. The beauty of the experimental results lies in the fact that, although the compounds are based on a complex chemistry, very clean anomalous universal exponents in both transport and thermodynamics are observed. In this paper, we do not detail the experimental result but rather refer the reader to the various reviews on the subject.^{2–5} One of the most famous example of universality is the linear-in- T resistivity observed in YbRh_2Si_2 fine tuned to quantum criticality with a small magnetic field parallel to the c axis. In this experiment, the linearity of the resistivity per-

sists on three decades of energy, which makes it one of the most robust anomalous exponents in strongly correlated materials.⁶ The coefficient of the specific heat $\gamma=C/T$ is found to increase when getting closer to the quantum critical point (QCP) without showing any sign of saturation. A logarithmic law is generally attributed to this increase, but in several cases, like for YbRh_2Si_2 , a divergence stronger than logarithmic is inferred from the data.³ Recently, another type of experiment showing quantum criticality has appeared with the observation of strong effective mass increase in He^3 bilayers.⁷ In this experiment, one layer of highly compressed solid He^4 is adsorbed on a graphite substrate, then another layer of solid He^4 , and on top of it, two layers of He^3 are adsorbed. The first layer of He^3 undergoes a transition toward a localized state at a finite filling factor. Measurements of the specific heat show a strong increase in the effective mass which is inversely proportional to the coverage, associated with a decrease in the coherence temperature in $(n-n_c)^{1,8}$, as the QCP is reached.

It is fair to say that this increasing body of fascinating experimental results is, at the present time, still mysterious. The biggest challenge for the theoretician is to account for the linear resistivity in three decades of energy in three dimensions of space. Such a result calls for a specific scattering process, from which the lifetime of the conduction electron would acquire the characteristic linear-in- T dependence. At the moment, no theory can produce a reasonable scenario accounting for linear-in- T resistivity down to zero temperature in three dimensions of space. The present paper, however, produces a very simple explanation for a resistivity linear in T but in the intermediate quantum critical regime: namely, above a finite (although quite small) energy scale.

Since the beginning of the history of heavy fermions, physicists have been struck by the intense magnetic nature of these materials. The presence of big atoms and big moments naively calls for magnetism. Moreover, magnetic interactions mediated by conduction electrons—called Ruderman–Kittel–Kasuya–Yosida (RKKY) interactions—are present in these materials.⁸ They compete with the formation of the Kondo singlets responsible for the condensation of the heavy Fermi liquid phase.^{9,10} For years, the magnetic nature of the mate-

rials was so overwhelming that it was a real surprise when the first heavy fermion superconductor was discovered.¹¹ Similarly, the competition between the magnetism and the formation of the Kondo singlets has been considered until recently to be the main physical forces at play in the Anderson lattice.^{12,13} In a completely natural way, the theory has first focused on QCPs separating a metallic magnetic phase from a metallic paramagnet.^{14–16} This is the simplest case of a QCP for itinerant electrons, usually called spin density wave (SDW) scenario. Here, the Fermi surface of the conduction electrons is destabilized by scattering through magnetic modes propagating through the metal: the paramagnons. A key concept in this theory is the dynamical exponent z . Since close to a QCP, quantum fluctuations are always relevant and the correlation in imaginary time has to be taken into account, which leads to an effective dimension $d+z$ larger than the d dimension of space. In practice, z is given by the structure of the bare paramagnon propagator. In the case of a transition toward an antiferromagnet (AF), the paramagnon propagator has the form $D^{-1}(q, i\omega_n) = c|\omega_n| + q^2$, where c is a constant. Hence, $z=2$ here. The theory then integrates the fermions out of the partition function^{14,15} step, which is not rigorously justified, to obtain an effective ϕ^4 Lagrangian in the $d+z$ dimensions. Since $z=2$ in the AF case, one is typically above the upper critical dimension of the model and the bosonic effective theory can be solved at the mean-field level. A better treatment of the model does not integrate the fermions out of the partition function but relies on an Eliashberg-type theory where the vertices are neglected and self-energies conserved.^{17,18} This theory is controlled in a rather artificial large N approximation where N multiplies the number of fermions. However, we use it in this paper every time we deal with a QCP of itinerant electrons, since it is the best technique available at the moment in that it avoids integrating the fermions out of the partition function, hence not missing any infrared (IR) divergence. Intense theoretical studies of the SDW scenario lead to the conclusion that some heavy fermion might fall into the universality class of the three dimensional (3D) AF, such as CeNi_2Ge_2 .¹⁹ Paramagnons, however, cannot account for strongly anomalous exponents such as a linear resistivity in 3D.

The search for new QCPs then started. New ideas emerged, such as the one of “deconfinement” of the heavy quasiparticle, close to the magnetic phase transition.³ Meanwhile, a phenomenological approach was proposed based on the observation that one can fit the NMR data for many compounds with two kinds of elementary excitations, which the authors called “two fluids.”²⁰ Although it is not clear whether it is really two “fluids” that are the good elementary excitations, the phenomenology looks robust and sets a landmark in the landscape of the field: the right microscopic theory should eventually reproduce the two fluid phenomenology. The first idea that a local mode appears at the QCP was given in Ref. 21 in the so-called “locally quantum critical scenario.” The strength of this idea is to have been the first to outline that “something local” has to appear at the QCP. In this theory, the local mode is of magnetic nature (a local spin). Its weakness, however, is that it requires the magnetic structure of the material to be purely two dimensions.²² Moreover, it appears to be very difficult to set it to the ex-

perimental test because the technique involved is not obviously transparent. To date, no experimental prediction has been made which would allow the community to accept or discard it.

Then, came the idea of a reconstruction of the Fermi surface at the quantum critical point, going with the idea of deconfinement.³ The first tractable effective field theory illustrating the ideas of deconfinement and of the Fermi surface reconstruction was given in Ref. 23. The authors used the Kondo–Heisenberg (KH) model and showed that, at some point in the phase diagram, there is a transition toward a spin liquid phase, which they called FL^* . At the transition, the Fermi surface reconstructs and one loses half of the charge carriers in the phase FL^* . Another way to look at the transition is to say that in the heavy Fermi liquid phase, the f electrons start to conduct, as was beautifully shown in Ref. 24. Apparently, the theory seemed to stand on much more solid grounds, since there was a tractable model on which to work. However, the treatment²³ suffered some insufficiencies. The most dramatic one is the complete lack of plausible experimental predictions. Apparently, the authors were not able to reproduce the linear-in- T resistivity, and the exponents they found for the anomalies in the specific heat coefficient did not match the experiments. Moreover, there was the problem of the phase FL^* . To have a “spin liquid” phase in any heavy fermion, compound appeared to be very unlikely. The most promising candidate for it was the system of He^3 bilayers, for which intensive numerical studies in the last decade^{25,26} have shown with very little doubt that, in its localized phase, adsorbed He^3 layers form a spin liquid.

II. RELATION TO PREVIOUS WORK AND STRUCTURE OF THE PAPER

This paper details the theory of the “Kondo breakdown” previously exposed into two letters.^{27,28} We describe the excitations around a selective Mott transition in the Anderson lattice using the simplest theoretical tool available, the $U(1)$ slave-boson gauge theory. Our goal is to cast the theory into the Eliashberg formalism with a careful treatment of the gauge invariance. To our knowledge, the Eliashberg technique is presented for a “deconfined” QCP, where the order parameter breaks a gauge symmetry (instead of a global symmetry). In particular, we present a study of the transport around such a QCP using the Ioffe–Larkin (IL) composition rule. We derive as well the most generic Ward identities (WIs) associated with the gauge symmetry.

First, note that the first study of a phase transition separating a spin liquid from a heavy Fermi liquid phase was performed for the Kondo lattice model with frustrated magnetism using the dynamical mean field theory (DMFT) technique.²⁹ Two other studies exist. Coleman *et al.*²⁴ showed that, at such a QCP in the KH model, there is a jump in the transport properties; the residual resistivity jumps at the QCP and the Hall conductivity as well. This follows from the fact that the f electrons start abruptly to conduct in the heavy Fermi liquid phase. These results come naturally in our formalism we thus agree with.²⁴ Our paper rederives their results using the simpler formalism of the IL composition rule.

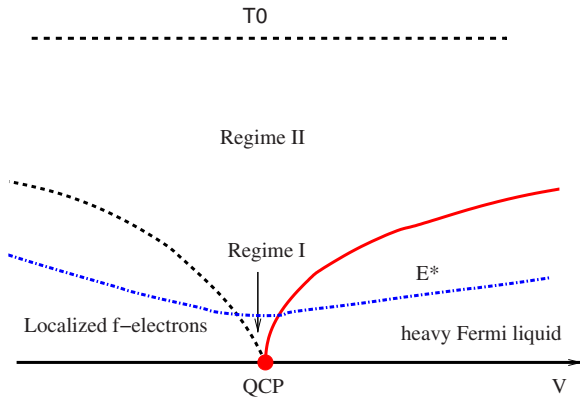


FIG. 1. (Color online) Schematic phase diagram for the selective Mott of the f electrons in the Anderson lattice. On the right, when the holons condense, is the heavy Fermi liquid phase, also called in this paper as the Higgs phase. On the left, where the holons are not condensed, is the localized phase for the f electrons. We do not analyze here the magnetic character of this phase but rather characterize it only by the fact that the f electrons localize. The QCP is multiscale as is shown by the scale E^* . Two regimes are of interest: (i) for $T \leq E^*$, the exponents depend on the shape of the Fermi surface, while (ii) for $T \geq E^*$, the exponents are universal and show quasilinear resistivity in $D=3$. T_0 is the upper energy cutoff, above which the entropy $R \ln 2$ per site is released.

The second study was done by Senthil *et al.*²³ The authors were the first to show that the volume of the Fermi surface jumps at the QCP. We agree with this result and with their observation that the thermodynamics, in the vicinity of the QCP, is dominated by the gauge fields. We disagree with their findings about the transport. Senthil *et al.*²³ claimed that, at very low energy, transport is dominated by the lifetime of the holons. One message of our study is that transport is dominated by the conduction electrons in all regimes.³⁰ This is imposed by the IL composition rule,

$$\rho = \rho_c + (\rho_f^{-1} + \rho_b^{-1})^{-1}, \quad (1)$$

which states that the resistance of the holons is in series with the resistance of the spinons and in parallel with the resistance of the conduction electrons.

Moreover, as already mentioned in Refs. 27 and 28, the general structure of the QCP is much richer than what was found in Ref. 23. This is depicted in Fig. 1. The first overlooked point is that the QCP is multiscale. By this, we mean that an intermediate energy scale is present at the QCP, separating two quantum critical regimes of universal exponents. The second overlooked point is that, in the intermediate energy regime, electrical conductivity simplifies, and one obtains a resistivity quasilinear in T in 3D. This regime is of main importance because it enables us to connect to experimental results and make predictions to test the theory. A first application of this regime to He^3 bilayers has already been given.³¹ The third overlooked point is that, at the mean-field level, a modulated solution of the heavy Fermi liquid state exists, analogous in structure to the modulations found for Fulde-Ferrell-Larkin-Ovchinnikov (FFLO) superconductivity.³² An analogous state was found in the study of

Chromium.³³ This state may be of relevance for the mysterious phase observed in CeCoIn_5 where the magnetic field is applied in the (ab) axis. Last, it appears that, in the case of the more physical model of the Anderson lattice with a small dispersion of the f electrons, the Kondo breakdown QCP coincides with a Mott transition of the f electrons.²⁸

The main advantage of this viewpoint is to simplify the discussion and to connect with other techniques available, such as dynamical mean field theory. DMFT studies can now be performed which will confirm or infirm in the short term the mean-field findings of a selective Mott transition in the periodic Anderson lattice model (PALM). Selective Mott transition has been previously studied in the context of multi-orbital Hubbard models,^{34–36} where transitions for various bands have been found.³⁷ This model differs from the PALM because of the absence of hybridization between the bands. Recent DMFT studies^{38–41} of the PALM tend to say that the selective Mott transition indeed exists, but the studies are not completely conclusive yet.

The second advantage is to link the discussion with the physics of high temperature superconductors.^{42–45} It is notorious that the conduction electrons undergo a Mott transition in the phase diagram of high T_c . Take a model with no frustration like the KH model on the square lattice. One can show formally that, in the localized phase, the model is equivalent to a Heisenberg antiferromagnet and that its ground state is an antiferromagnet. This point was actually made in Ref. 23. Although this statement is formally simple, it is very difficult to obtain within the slave-boson technique. In two dimensions, for high T_c superconductors, one can advocate that the spin liquid naturally reconfines under the effect of gauge fluctuations.⁴⁵ We do not have this latitude in 3D where gauge fluctuations are benign and can be treated within a noncompact formalism. A better route toward the AF ground state is probably to allow the system to have both AF order and spin liquid and then study the issue of re-confinement in that case. Similar studies have been performed in the early days of high T_c (Ref. 46) but have not yet been done for the Anderson lattice.

On the theory side, the Kondo breakdown QCP suffers as well from its own weaknesses. We outline the main one, in our view, which is that this fixed point relies on the presence of a spin liquid at the transition. This spin liquid is described in terms of the massless spinons, and the model is very sensitive to the Fermi surface of the spinons. To be precise, the exponents obtained using, for example, the uniform spin liquid are different from the ones obtained using a nodal spin liquid. Whether the linear-in- T resistivity found in the intermediate phase survives the “spinology” is still an open question. A related question is to ask whether the $U(1)$ gauge theory used in the description of the Kondo breakdown is the adequate tool to describe the approach to a Mott transition. Are the elementary excitations correctly captured within this technique? This question is of broad interest and is as well at the heart of the physics of high temperature superconductors.

The paper is organized as follows. In Sec. III, we recall the model and introduce the slave-boson effective Lagrangian. Sections IV and V are devoted to the mean-field approximation. Precisely, in Sec. IV, we describe the mean-field approximation, showing the presence of the QCP at $T=0$. In

Sec. V, we recall the possibility of another mean-field solution: a modulated order parameter in the heavy Fermi liquid phase. In Secs. VI and VIII, we study the fluctuations. We first start, in Secs. VI and VII, by introducing the amplitude and gauge fluctuations within a “naive” random-phase approximation (RPA). In Sec. VIII, we expose the Eliashberg formalism which links self-consistently the amplitude and gauge fluctuations and is the best available tool to study QCPs of that type. Precisely, in Sec. IV, we study the fluctuations of the amplitude of the order parameter, showing the different regimes of quantum criticality. In Sec. VII, we introduce the gauge fluctuations, give the form of their propagator, and detail the gauging out of the theory. In Sec. VIII, we recall the principles of the Eliashberg theory and recast our study of the fluctuations in this framework. We then turn to electrical transport. In Sec. IX, we compute the IL composition rule for the conductivity around the QCP and derive the various transport lifetimes in the low temperature regime. In Sec. X, we focus on the intermediate regime and give the arguments for the quasilinear resistivity in $D=3$. In Sec. XI, we give a summary of the thermodynamics and transport in this model. Finally, in Sec. XII, we present the conclusions and a criticism of the work.

Appendixes A and H are devoted to some technical details. Precisely, in Appendix A, we give the calculation of the integrals used at the mean-field approximation. In Appendix B, we give the details of the evaluation of the vertices, which justify the Eliashberg treatment. In Appendix D, we give an alternative, very simple derivation of the IL composition rules. In Appendix E, we give the evaluation of the bosonic polarization used in the form of the gauge propagator as well as in the holon transport lifetime. In Appendix F, we give a field theoretic treatment of the Ward identities of this gauge theory, relating any p -leg vertex to a $(p-1)$ -leg one. We show as well in the most general way how the gauge symmetry protects the masses of the gauge fields in the Coulomb phase and how the mass is generated in the Higgs phase. In Appendix G, we give a direct check of the cancellation of the mass in the Coulomb phase at the first order in the perturbation theory. Last, in Appendix H, we give the derivation of $\text{Im } \Sigma_c$ and particularly show that the logarithm in $D=3$ has a thermal origin.

III. MODEL

In order to study the Mott localization of the f electrons in the Anderson lattice, we must first allow them to disperse. A small dispersion of the f electrons is naturally present in the most physical models for heavy fermions. The reason why it is rarely included in the starting Hamiltonians¹⁰ is that, in the study of the heavy Fermi liquid phase, the f electron dispersion is irrelevant compared to the formation of the Kondo singlets, and one can safely approximate the narrow band by a flat one. We thus start with the Anderson lattice model, with a small dispersion of the f band,

$$H = \sum_{i,j\sigma} [c_{i\sigma}^\dagger t_{ij} c_{j\sigma} + \tilde{f}_{i\sigma}^\dagger (\alpha t_{ij} + E_0 \delta_{ij}) \tilde{f}_{j\sigma}] + \sum_{i,\sigma} [(V \tilde{f}_{i\sigma}^\dagger c_{i\sigma} + \text{H.c.}) + U \tilde{n}_{f,i}^2 + U_{fc} \tilde{n}_{f,i} n_{c,i}], \quad (2)$$

where α is a small parameter, σ is a spin index belonging to

the SU(2) representation, $t_{ij}=t$ is the hopping term taken as a constant, V is the hybridization between the f and c bands, and E_0 is the energy level of the f electrons. $\tilde{n}_{f,i} = \sum_{\sigma} \tilde{f}_{i\sigma}^\dagger \tilde{f}_{i\sigma}$ and $n_{c,i} = \sum_{\sigma} c_{i\sigma}^\dagger c_{i\sigma}$ are the operators describing the particle number. We first study Eq. (2) in the limit of very large on-site Coulomb repulsion U . U_{fc} accounts for the Coulomb interaction between the f and c electrons; although $U_{fc} \ll U$, it must be taken into account in the derivation of the effective theory. Here, we go beyond the treatment of Ref. 28 and include as well in the model the RKKY interactions mediated by the conduction electrons. The starting Hamiltonian writes

$$H = \sum_{i,j\sigma} [c_{i\sigma}^\dagger t_{ij} c_{j\sigma} + \tilde{f}_{i\sigma}^\dagger (\alpha t_{ij} + E_0 \delta_{ij}) \tilde{f}_{j\sigma}] + \sum_{i,\sigma} [(V \tilde{f}_{i\sigma}^\dagger c_{i\sigma} + \text{H.c.})] + \sum_{\langle ij \rangle} \left[J_0 \left(\tilde{\mathbf{S}}_{f,i} \cdot \tilde{\mathbf{S}}_{f,j} - \frac{n_{fi} n_{fj}}{4} \right) \right] + \sum_{\langle ij \rangle} [J_{\text{RKKY}} (\tilde{\mathbf{S}}_{f,i} \cdot \tilde{\mathbf{S}}_{f,i} \cdot \mathbf{S}_{c,j})], \quad (3)$$

where J_0 and J_1 are determined by the second order perturbation theory in large $U/(\alpha t)$ and $U_{fc}/(\alpha t)$ and J_{RKKY} is determined by second order perturbation theory in small V/D , where D is the bandwidth of the conduction electrons. One obtains $J_0 = 2(\alpha t)^2/U$, $J_1 = 2(\alpha t)^2/U_{fc}$, and $J_{\text{RKKY}} = \rho_0 V^2$ where ρ_0 the density of states of the conduction electrons. $\tilde{\mathbf{S}}_f = \sum_{\alpha\beta} \tilde{f}_{i\alpha}^\dagger \vec{\sigma}_{\alpha\beta} \tilde{f}_{i\beta}$ ($\mathbf{S}_c = \sum_{\alpha\beta} c_{i\alpha}^\dagger \vec{\sigma}_{\alpha\beta} c_{i\beta}$) and $\vec{\sigma}$ is the Pauli matrix. The summation over $\langle ij \rangle$ can run on first nearest neighbors as well as second, third, etc., nearest neighbors. Here, we simplify the discussion by restricting all spin interactions to first nearest neighbors only, hence restricting our attention to the commensurate AF case. It has to be kept in mind that this is not the most generic situation and that frustration naturally appears in this model.

We then take the $U \rightarrow \infty$ limit of Eq. (3). We account for the constraint of no double occupancy through a Coleman⁴⁷ set of bosons (b^\dagger, b) enslaved to a constraint on each site, $\sum_{\sigma} \tilde{f}_{i\sigma}^\dagger \tilde{f}_{i\sigma} + b_i^\dagger b_i = 1$. We make at each site the transformation

$$\tilde{f}_{i\sigma} \rightarrow f_{i\sigma} b_i^\dagger, \quad (4)$$

where the f^\dagger -creation operators are called “spinons” and the b^\dagger “holons.” The physical electron \tilde{f} splits into a holon and a spinon under transformation (4). We notice that, upon this transformation, the slave boson drops out of all bilinear products of fields at the same site. Indeed, one can explicitly show that at site i

$$f_{i\sigma}^\dagger b_i b_i^\dagger f_{i\sigma} |0\rangle = f_{i\sigma}^\dagger f_{i\sigma} |0\rangle = 0, \quad (5)$$

$$f_{i\sigma}^\dagger b_i b_i^\dagger f_{i\sigma} |\sigma\rangle = f_{i\sigma}^\dagger f_{i\sigma} |\sigma\rangle = n_{f,i\sigma} |\sigma\rangle$$

Another way to see this is to apply the constraint inside the operator,

$$f_{i\sigma}^\dagger b_i b_i^\dagger f_{i\sigma} = (1 - n_b) f_{i\sigma}^\dagger f_{i\sigma} = n_{f,i} f_{i\sigma}^\dagger f_{i\sigma} = f_{i\sigma}^\dagger f_{i\sigma}. \quad (6)$$

The last line is obtained by observing that the constraint of no double occupation is equivalent to $n_{fi}^2 = n_{fi}$.

The effective Lagrangian is then

$$\begin{aligned} \mathcal{L} = & \sum_{i,j\sigma} \{c_{i\sigma}^\dagger(\partial_\tau\delta_{ij} + t_{ij})_{j\sigma} + f_{i\sigma}^\dagger[b_i\alpha t_{ij}b_j^\dagger + (\partial_\tau + E_0 + \lambda_i)\delta_{ij}]f_{j\sigma}\} \\ & + \sum_i b_i^\dagger(\partial_\tau + \lambda_i)b_i - \lambda + \sum_{i,\sigma} (Vf_{i\sigma}^\dagger b_i c_{i\sigma} + \text{H.c.}) \\ & + \sum_{\langle ij \rangle} (J\mathbf{S}_{f,i} \cdot \mathbf{S}_{f,j} + J_1\mathbf{S}_{f,i} \cdot \mathbf{S}_{c,j}), \end{aligned} \quad (7)$$

where the constraint has been implemented through a Lagrange multiplier λ_i . Note that the spin operator $\mathbf{S}_f = \sum_{\alpha\beta} f_{i\alpha}^\dagger \vec{\sigma}_{\alpha\beta} f_{i\beta}$ is now expressed solely in terms of the spinons and thus is insensitive to the slave bosons.

In the following, we consider a ‘‘large N ’’ extension of Lagrangian (7) by enlarging the spin group from $SU(2)$ to $SU(N)$. The indices σ now belong to the $SU(N)$ group.

IV. MEAN-FIELD APPROXIMATION

In the mean-field approximation, we minimize the effective action with four fields: λ , b , ϕ_0 , and σ_0 , where a static and uniform approximation is made on all fields. ϕ_0 is the uniform spin liquid parameter, which decouples the short range AF interaction $J\mathbf{S}_{f,i} \cdot \mathbf{S}_{f,j} \rightarrow \phi_0 \sum_{i,\sigma} (f_{i\sigma}^\dagger f_{i\sigma} + \text{H.c.}) - N\phi_0^2/J$. σ_0 is the uniform field which decouples the induced Kondo-type interaction $J_1\mathbf{S}_{f,i} \cdot \mathbf{S}_{c,j} \rightarrow \sigma_0 \sum_{i,\sigma} (f_{i\sigma}^\dagger c_{i\sigma} + \text{H.c.}) - N\sigma_0^2/J_1$. The minimization of the free energy leads to the following mean-field equations:

$$T \sum_{k,\sigma,\omega_n} \alpha \epsilon_k G_{ff} + \frac{V}{b} \sum_{k,\sigma,\omega_n} G_{fc} + \epsilon_f - E_0 = 0,$$

$$T \sum_{k,\sigma,\omega_n} G_{fc} + N\sigma_0/J_1 = 0,$$

$$T \sum_{k,\sigma,\omega_n} (\epsilon_k/D) G_{ff} + N\phi_0/J = 0,$$

$$b^2 + T \sum_{k,\sigma,\omega_n} G_{ff} = N/2,$$

where ϵ_k is a typical dispersion of the conduction electrons, $\epsilon_f = E_0 + \lambda$, and the dispersion of the spinon band is taken to be $\epsilon_k^0 = [ab^2 + (\phi_0/D)]\epsilon_k + \epsilon_f$. We have the following Green's functions:

$$\begin{aligned} G_{ff} &= \frac{i\omega_n - \epsilon_k}{(i\omega_n - \epsilon_k)(i\omega_n - \epsilon_k^0) - (Vb + \sigma_0)^2}, \\ G_{fc} &= \frac{Vb + \sigma_0}{(i\omega_n - \epsilon_k)(i\omega_n - \epsilon_k^0) - (Vb + \sigma_0)^2}, \\ G_{cc} &= \frac{i\omega_n - \epsilon_k^0}{(i\omega_n - \epsilon_k)(i\omega_n - \epsilon_k^0) - (Vb + \sigma_0)^2}. \end{aligned} \quad (8)$$

The mean-field equations are solved in the case of a linearized bandwidth and for $N=2$; energy scales extracted from the mean-field studies are as well written for $N=2$. The sum-

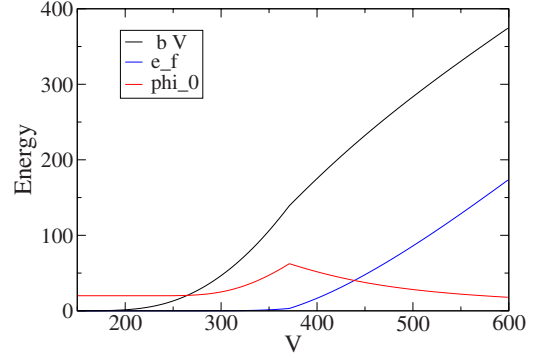


FIG. 2. (Color online) Effective hybridization Vb (black curve), the f -band chemical potential $\epsilon_f = E_0 + \lambda$ (blue curve), and $20\phi_0$ (red curve), as a function of V . The electron bandwidth is $D=1000$. The chemical potential $\mu=0$, the ratio of f and c masses is $\alpha=0.1$. ϕ_0 is evaluated self-consistently around finite RKKY value of $10^{-3}D$. The f -energy level is $E_0 = -500$. The mean-field equations are solved for $N=2$. The effect of the field σ is negligible, hence not shown in the figure.

mations over (k, ω_n) can then be performed analytically and are given in Appendix A; the set of resulting equations is then solved numerically. Since the interaction $J_1\mathbf{S}_{f,i} \cdot \mathbf{S}_{c,j}$ generates some additional Kondo coupling, it is not obvious that a Mott transition- a point in the phase diagram where $b=0$ occurs at finite V . However, this is what happens, the additional Kondo coupling σ_0 being itself driven to zero at the transition. The result is displayed in Fig. 2.

We can study analytically the nature of the fixed point by expanding the mean-field [Eq. (8)] around

$$\sigma_0 = 0,$$

$$b = 0,$$

$$|\phi_0| = cJ, \quad c \approx 0.1. \quad (9)$$

From the first equation, we get that

$$\Pi_{fc}(0) + (\epsilon_f - E_0)/V^2 \approx 0,$$

where

$$\Pi_{fc}(0) = T \sum_{k,\omega_n,\sigma} \frac{1}{(i\omega_n - \epsilon_k)(i\omega_n - \epsilon_k^0)}. \quad (10)$$

Using, for the conduction electrons and the spinons, linearized dispersions of the form $\epsilon_k = v_F(k - k_F)$ and $\epsilon_k^0 = v_0(k - k_0)$, with $v_0 = 2\phi_0/k_F$, one obtains

$$\Pi_{fc}(0) = N\rho_0 \frac{\log(\alpha')}{(1 - \alpha')}, \quad (11)$$

with

$$\alpha' = ab^2 + \phi_0/D. \quad (12)$$

One can convince oneself that the fixed point occurs when $\phi_0 = D \exp[\frac{E_0}{N\rho_0 V^2}]$. One recognizes here the typical Kondo scale of the problem.^{48,49} Hence,

$$J_{\text{crit}} = D \exp\left[\frac{E_0}{N\rho_0 V^2}\right]. \quad (13)$$

One sees that the location of the QCP in the phase diagram depends crucially on the spin liquid parameter J . Moreover, it is important for the stability of the mean-field equations that the bandwidth stays finite when $b \rightarrow 0$. This is achieved with the uniform spin liquid parameter ϕ_0 being finite at the transition. The mean-field equations are of little help to determine the nature of the localized phase where $b=0$. In the simplified scheme we have taken, this phase is a uniform spin liquid— ϕ_0 being finite and uniform. The spinons can, however, have some other symmetries, and it would be useful, for example, to determine the location of the transition when spinons with a nodal Fermi surface are used. One can as well allow for AF order in the localized side and study the stability of the phase diagram. This is the program for future work.

V. MODULATIONS OF THE ORDER PARAMETER

In Sec. IV, we have naturally considered that the order parameter b was ordering at $q=0$. This issue has to be reconsidered keeping in mind the nature of the spinon Fermi surface. In this section, we review for completeness the results obtained in Ref. 27. At the QCP, the effective mass of the order parameter writes

$$D_b^{-1}(q,0) = m_b, \quad (14)$$

$$m_b(q) = \rho_0[-E_0 + V^2\Pi_{fc}(q)],$$

where $\Pi_{fc}(q)$ is the static fc polarization, taken at finite momentum q but zero frequency. At the QCP, the minimum of the effective mass determines the ordering wave vector. Two situations are to be considered. First, if both the f and c bands are electronlike, $\Pi_{fc}(q)$ obtains its minimum at $q_0=0$. Note that in that case, the curvature of the Fermi surface has to be included to see the minimum. Second, if one band is electronlike but the other one is holelike, then the situation is analogous to the FFLO ordering in superconductors³² or to charge density waves in Ref. 33. At the QCP, the ordering wave vector is at $q_0 \approx 1.2q^*$, where

$$q^* = |k_F - k_0| \quad (15)$$

is the difference between the Fermi wave vectors of the two species. The determination of the ordering wave vector inside the ordered phase is much more involved than at the QCP. It led to a full literature in the case of FFLO superconductivity.³² One generally expects a first order transition toward a uniform order inside the ordered phase. Here, the situation is rather more complex than in the FFLO case because the order parameter b carries one quantum of gauge charge. Gauging out the theory, even at the mean-field level, is required to deduce the observable quantities. This study definitely deserves more work. Particularly, it would be

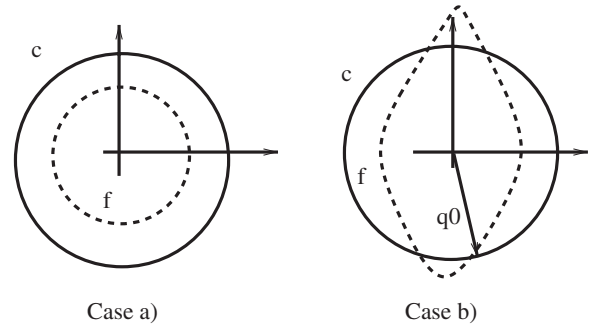
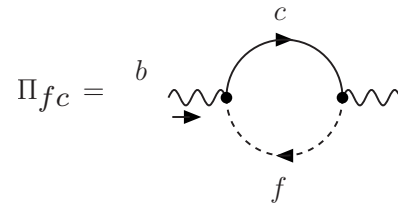


FIG. 3. Illustration of the two typical cases of interest. In case (a), the two Fermi surfaces of the spinons and conduction electrons are centered and there is a gap between them; in case (b), the two Fermi surfaces intersect.

interesting to see what kind of superconductivity occurs in a Kondo phase where the hybridization is modulated in space.

VI. AMPLITUDE FLUCTUATIONS

In Secs. VII and VIII, we describe the RPA evaluation of the amplitude and gauge fluctuations. The fluctuations are studied in the case of the order parameter condensing at $q=0$. The fluctuations of the amplitude of the order parameter are more complex than what was considered in Ref. 23 since the order parameter is coupled to two types of fermions: the f spinons and the conduction electrons. Neglecting for the moment the effect of gauge fluctuations, within the RPA, the polarization is similar to a Lindhard function, but with two different types of fermions,



$$D_b^{-1}(q, i\Omega_n) = \rho_0[-i\Omega_n + \delta + aq^2 + \Pi_{fc}(q, i\Omega_n)], \quad (16)$$

with $a = -N \log(\alpha') / [(1 - \alpha')^2 k_F^2]$, the bosonic mass $\delta = -E_0$ comes from the mean-field equations, and ρ_0 is the density of states of the conduction electrons. Note that, in our definition, Π_{fc} is the “dynamical” polarization, corresponding to the IR sector. In the text, we use this definition for every polarization. Let us here evaluate Π_{fc} . There are two cases of interest, as shown in Fig. 3. Depending whether the Fermi surface of the spinons and conduction electrons intersect or not, we have two forms for the amplitude propagator. Let us start with case (a) where there is a gap between the spinon and electron Fermi surfaces. Using linearized bands, the polarization can be computed analytically and we get at $T=0$

$$\begin{aligned}
\Pi_{fc}(q, i\Omega_n) &= \frac{N\rho_0}{4\pi} \int d\epsilon d\omega d\cos\theta \frac{1}{(i\omega + i\Omega_n - \epsilon - v_F q \cos\theta)(i\omega - \alpha\epsilon - \alpha v_F q^*)}, \\
&= \frac{-\rho_0}{2v_F \alpha' q (1-\alpha')} \{ [-\alpha' i\Omega_n + \alpha' v_F (q - q^*)] \log[-i\alpha' \Omega_n + \alpha' v_F (q - q^*)] - [-\alpha' i\Omega_n + \alpha' v_F (-q - q^*)] \\
&\quad \times \log[-i\alpha' \Omega_n + \alpha' v_F (-q - q^*)] - [i\Omega_n + \alpha' v_F (q - q^*)] \log[-i\Omega_n + \alpha' v_F (q - q^*)] + [i\Omega_n + \alpha' v_F (-q - q^*)] \\
&\quad \times \log[-i\Omega_n + \alpha' v_F (-q - q^*)] \}. \tag{17}
\end{aligned}$$

We see that an additional scale q^* naturally emerges from the polarization. q^* is the difference between the Fermi wave vectors of the f spinons and c electrons. Here, we have taken both the spinon Fermi surface and the electron Fermi surface to be spherical and centered with respect to each other; hence, q^* is isotropic. We define the energy scale for $N=2$ by

$$E^* = 0.1 \alpha' D \left(\frac{q^*}{k_F} \right)^3. \tag{18}$$

We can expand Eq. (17) in four different regimes.

(i) For $q \leq q^*$, $|\Omega_n| \leq E^*$, we have

$$D_b^{-1}(q, i\Omega_n) \approx \rho_0 \left[\tilde{\delta} + aq^2 - N \frac{i\Omega_n}{\alpha' v_F q^*} \right], \tag{19}$$

with $\tilde{\delta} = -E_0 + \rho_0 V^2 \log \alpha' / (1 - \alpha')$.

(ii) For $q \leq q^*$, $E^* \leq |\Omega_n|$, we have

$$D_b^{-1}(q, i\Omega_n) \approx \rho_0 \left[\tilde{\delta} + aq^2 + N \frac{\log|\Omega_n|}{\alpha' v_F q^*} \right]. \tag{20}$$

(iii) For $q \geq q^*$, $\alpha' v_F q \leq |\Omega_n| \leq v_F q$, we have

$$D_b^{-1}(q, i\Omega_n) \approx \rho_0 \left[\tilde{\delta} + aq^2 + N \frac{\log|\Omega_n|}{\alpha' v_F q} \right]. \tag{21}$$

(iv) For $q \geq q^*$, $v_F q \leq |\Omega_n|$, we have

$$D_b^{-1}(q, i\Omega_n) \approx \rho_0 \left[\tilde{\delta} + aq^2 + N \frac{|\Omega_n|}{\alpha' v_F q} \right]. \tag{22}$$

Note the peculiar form of the boson propagator, where the different sectors are not in the same footing in large N .⁵⁰ We do not know anyway how to avoid this problem within the Eliashberg theory, and that is why we call it a large N expansion rather than a large N limit. We refer the reader to Refs. 18 and 51 for further details about this and to Sec. VII, just mentioning here that the merit of the Eliashberg theory is to capture all the frequency divergences within the leading and second leading orders in $1/N$. To each regime, one can associate a different dynamical exponent. In regime (i), the dynamical exponent is $z=2$ and the propagator corresponds to an undamped bosonic mode. In regime (ii), the dynamical exponent is $z=\infty$. In regime (iii), we get $z=1$. Finally, regime (iv) has $z=3$. It was shown that the spectral weight in the (Ω, q) space is most entirely centered in regime (iv) where $z=3$.²⁷ This feature is illustrated in Fig. 4.

Physical arguments enable us to simplify the discussion. At low momentum and low energy, the particle-hole continuum is gapped due to the mismatch of the two Fermi surfaces. There is propagation of a single boson mode with exponent $z=2$ [Eq. (19)]. At high momentum and high energy, one can neglect the mismatch of the two Fermi surfaces; the two fermion species behave as if they were identical. The polarization behaves like a Lindhard function [Eq. (22)] with $z=3$; this form is typical of a $q=0$ phase transition.

As we have shown above, an energy scale E^* is present in the quantum critical regime, separating two regimes with universal exponents. In the low energy regimes $T \ll E^*$, the fluctuations of the amplitude are gapped and thermodynamics is dominated by gauge fluctuations. For $T \gg E^*$, the thermodynamics is in the universality class of the ferromagnet with $z=3$.

One can ask the question “why is E^* so low.” To answer it, we give an estimate of E^* . One can first identify $\alpha' D$ with the temperature T_0 at which the entropy $R \ln 2$ is released in the Anderson lattice. This scale is seen experimentally in

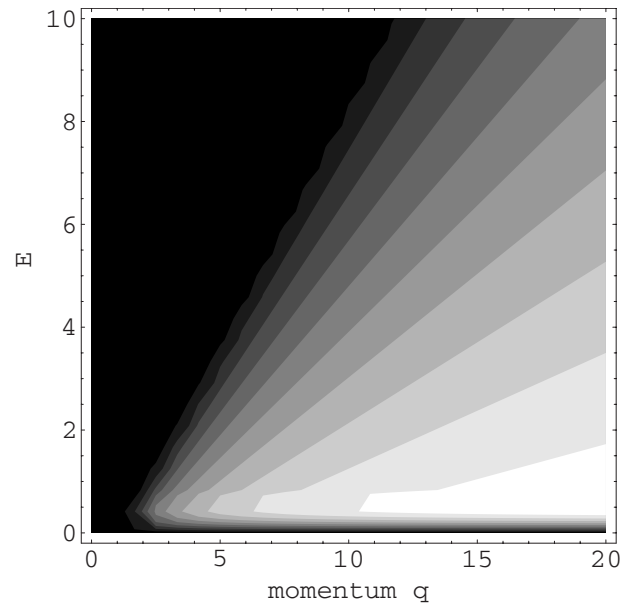


FIG. 4. Spectral weight of the Π_{fc} polarization in the (q, ω) plane. We have taken $q^*=1$, $v_F=1$, and $\alpha'=0.01$. We see that the weight is concentrated in regime II ($z=3$) for $q \geq q^*$, where one has particle-hole damping.

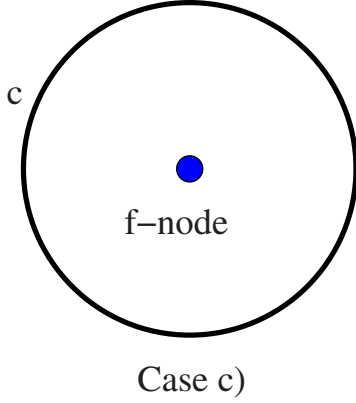


FIG. 5. (Color online) The third case of interest, where the spinon f Fermi surface is nodal, like for the U(1) gauge theory of the one band Hubbard model, in $D=2$. This is in the same universality class as case (a).

every compound as a bump into the thermodynamic and transport observables. For $T \geq \alpha'D$, the spinons lose their dispersion; hence, one can consider that they behave as free spins and that the entropy $R \ln 2$ is released. This observation fixes the scale T_0 to be roughly 24 K for a compound such as YbRh_2Si_2 and 50 K for CeCoIn_5 . We see from Eq. (18) that even for very large q^* , E^* is already an order of magnitude lower than T_0 , which makes it a small scale already. Next, depending on the form of the spinon Fermi surface, q^* can be as small as $0.1k_F$, in which case the scale E^* is of the order of 10 mK, which means it is not experimentally reachable. The fact that E^* relies on the imponderable form of the spinon Fermi surface is assuredly the weak point of this theory.

To illustrate this point, we look at the more generic case (b), where the spinon Fermi surface and the electron Fermi surface intersect in two “hot lines.” Since the anisotropy is broken, we define a new q^* as

$$q^* = \max_{(\theta, \phi)} [k_F - k_0], \quad (23)$$

where the maximum is taken over angular variables on the Fermi surface. In this case, regime (iv) is unchanged, but regime (i) is different, since the particle-hole continuum is not gapped. The boson propagator in regime (i) is now

$$D_b^{-1}(q, i\Omega_n) \simeq \rho_0 \left[\tilde{\delta} + aq^2 + Nc \frac{|\Omega_n|}{\alpha' v_F q_0} \right], \quad (24)$$

where q_0 is the modulus of the wave vector at which the two Fermi surfaces intersect and c is a coefficient depending on the shape of the Fermi surfaces. We see that the propagator still has the dynamical exponent $z=2$, but it is now damped; hence, in the same universality class as a 3D antiferromagnetic SDW QCP. We note that the change in the spinon Fermi surface between case (a) and case (b) did not affect the regime for $T \geq E^*$. Although we cannot prove that this result is general, we illustrate it with considering a third case where the f -spinon Fermi surface is nodal in two dimensions, as shown in Fig. 5. This case is interesting because it is the exact analog to the description of the one band Hubbard

model within the U(1) or SU(2) slave-boson gauge theory.^{42,45} One can show that the amplitude propagator is formally equivalent to case (a), where the two Fermi surfaces are gapped. Hence, in that case as well, the regime with $T \geq E^*$ is unaffected by the form of the spinon Fermi surface, although E^* is supposedly bigger than in case (a), since q^* and k_F are of the same order of magnitude. In conclusion, the regime $T \geq E^*$ depends on the existence of the spinon Fermi surface but not on its shape.

VII. GAUGE FLUCTUATIONS

The order parameter of our phase transition is not a macroscopic order parameter but relies on the condensation of a gauge boson carrying one quantum of charge of the gauge invariant theory. We study here the U(1) local invariance of the Lagrangian. For clarity, we start with the evaluation of the polarization of the gauge fields within RPA. The WIs constraining the masses are given in Appendix F. We start with the version of Eq. (3) after having performed the Hubbard–Stratonovich transformation,

$$\begin{aligned} \mathcal{L} = & \sum_{i,j\sigma} \{c_{i\sigma}^\dagger (\partial_\tau \delta_{ij} + t_{ij}) c_{j\sigma} + f_{i\sigma}^\dagger [b_i \alpha t_{ij} b_j^\dagger \\ & + (\partial_\tau + E_0 + i\lambda_i) \delta_{ij}] f_{j\sigma}\} + \sum_i b_i^\dagger (\partial_\tau + i\lambda_i) b_i - i\lambda_i \\ & + \sum_{i,\sigma} [(Vb_i + \sigma_i) f_{i\sigma}^\dagger c_{i\sigma} + \text{H.c.}] + \frac{N}{J} \sum_{\langle ij \rangle} |\phi_{ij}|^2 + \frac{N}{J_1} |\sigma_i|^2 \\ & + \sum_{\langle ij \rangle \sigma} (f_{i\sigma}^\dagger f_{i\sigma} \phi_{ij} + \phi_{ij}^* f_{j\sigma}^\dagger f_{j\sigma}). \end{aligned} \quad (25)$$

Under the gauge transformation,

$$\begin{aligned} f_i & \rightarrow f_i e^{-i\theta_i}, \\ b_i & \rightarrow b_i e^{i\theta_i}, \\ \sigma_i & \rightarrow \sigma_i e^{i\theta_i}, \\ \lambda_i & \rightarrow \lambda_i + \partial_\tau \theta_i, \\ \phi_{ij} & \rightarrow \phi_{ij} e^{i\theta_i - \theta_j}, \end{aligned} \quad (26)$$

Lagrangian (25) acquires a total derivative $\mathcal{L}(\tau) \rightarrow \mathcal{L}(\tau) - i \sum_i (\partial_\tau \theta_i)$ which is a multiple of $2i\pi$ and thus leaves the Lagrangian invariant. The above Lagrangian is thus invariant under a U(1) local—or gauge—symmetry. In the mean-field treatment above, we have considered that the Hubbard–Stratonovich fields can be taken at their saddle points $\langle \sigma_i \rangle = \sigma_0$, $\langle \lambda_i \rangle = i\lambda$, $\langle b_i \rangle = b$, and $\langle \phi_{ij} \rangle = \phi_0$, and we have neglected the fluctuations of the phases of the field as well as of the amplitudes. It is safe to assume that the amplitude fluctuations of ϕ_{ij} are gapped since ϕ_0 does not vanish through the phase diagram. At the QCP, however, the amplitude fluctuations of b_i and σ_i become massless. Another issue is the phase of the gauge fields. In order to study them, it is convenient to take the continuum limit in Lagrangian (25). For this, we write $\phi_{ij} = \phi_0 e^{i\alpha_{ij}}$ and now the second and third terms

in Eq. (25) describe spinons and holons in the presence of the fictitious electromagnetic field \mathbf{B} associated with the vector potential \mathbf{a} with $\int_i^j \mathbf{a} \cdot d\mathbf{l} = \mathbf{a}_{ij}$.^{42,45} We then coarse grain Lagrangian (25) to obtain the continuous limit

$$\begin{aligned} \mathcal{L}(\mathbf{r}, \tau) = & \sum_{\sigma} \int d\mathbf{r} c_{\sigma}^{\dagger} \left(\partial\tau - \frac{\nabla^2}{2m} - \mu \right) c_{\sigma} \\ & + f_{\sigma}^{\dagger} \left(\partial\tau - \frac{(\nabla + ie\mathbf{a}/c)^2}{2m_f} + \epsilon_f + ia_0 \right) f_{\sigma} \\ & + b^{\dagger} \left(\partial\tau - \frac{(\nabla + ie\mathbf{a}/c)^2}{2m_b} + \lambda + ia_0 \right) b + \frac{N}{J_1} \sigma(\mathbf{r})^2 \\ & + \frac{N}{J} \phi_0^2 + \sum_{\sigma} \int d\mathbf{r} [(Vb + \sigma) f_{\sigma}^{\dagger} c_{\sigma} + \text{H.c.}]. \end{aligned} \quad (27)$$

When the order parameter $b + \sigma/V$ condenses, the gauge field \mathbf{a} acquire a gap proportional to $(b + \sigma/V)$ according to the rules for the condensation of a Higgs boson.⁵² This phenomenon is responsible for the Meissner effect in the case of a superconductor. In Appendix F, we derive the generation of the mass using the Ward identities associated with the gauge invariance.

A nontrivial issue is the gauging out of the theory. The slave-boson representation required the use of additional fields, hence the field theory is redundant and some gauge fluctuations can be factorized out of the partition function. Since one deals with a U(1) gauge theory, one gauge fixing constraint only is required. When gauging out the theory, it is convenient to chose the radial gauge for the Higgs phase—also called here as “heavy Fermi liquid,” which follows previous studies of the Kondo impurity^{47,53} and of the Kondo lattice.⁹ Namely, we choose the order parameter to be real, with, for example,

$$b + \sigma/V = |b + \sigma/V|. \quad (28)$$

This constraint is alternatively called the “physical gauge” in field theory, since the gapping of the gauge fields in the Higgs phase is transparent in this gauge.⁵² When the order parameter vanishes, in the so-called Coulomb phase, it is clever to use the Coulomb gauge imposing the condition

$$\nabla \cdot \mathbf{a} = 0, \quad (29)$$

so that the vector fields become purely transverse. In the Coulomb gauge, the scalar fields ($\mu=0$) and vector fields decouple; the scalar fields are massive, which are nothing than the density-density correlation function, while the mass of the vector fields remains massless [see Eq. (E9)]. The polarization of the vector fields gives rise to a Reizer singularity⁵⁴ described below. Of course, formally all gauge fixings should be equivalent, and there is no deep reason to choose one constraint rather than the other. However, if, for example, one tries to work with the radial gauge in the Coulomb phase, lots of divergences appear which have to cancel at the end for physical quantities. The reason is that radial coordinates are ill-defined when the radius vanishes (here, the radius is the modulus of the order parameter $|b + \sigma/V|$). Some divergences are then hidden in the Jacobian of the

transformation. We are not aware of any field theoretic treatment of this case for condensed matter systems.

At the QCP, we thus work in the Coulomb gauge where the vector fields have the purely transverse form,

$$D_{ij}^{-1}(q, i\Omega_n) = \Pi(q, i\Omega_n) (\delta_{ij} - q_i q_j / q^2), \quad (30)$$

with

$$\begin{aligned} \Pi(q, i\Omega_n) = & -\frac{1}{2} \langle T_{\tau} [\mathbf{J}_{f,i}(\mathbf{r}, \tau) \mathbf{J}_{f,j}(0, 0)] \rangle + \delta_{ij} \frac{\rho_0}{2m_f} \delta(\mathbf{r}) \delta(\tau) \\ & -\frac{1}{2} \langle T_{\tau} [\mathbf{J}_{b,i}(\mathbf{r}, \tau) \mathbf{J}_{b,j}(0, 0)] \rangle + \delta_{ij} \frac{\rho_0}{2m_b} \delta(\mathbf{r}) \delta(\tau). \end{aligned} \quad (31)$$

The first term in Eq. (31) corresponds to the paramagnetic contribution, while the second term is the diamagnetic part. \mathbf{J}_f is the current operator defined as $\mathbf{J}_f = i/(2m_0)[f^{\dagger} \nabla f - (\nabla f^{\dagger}) f]$ and $\mathbf{J}_b = i/(2m_b)[b^{\dagger} \nabla b - (\nabla b^{\dagger}) b]$. After Fourier transforming, the polarization can be written as

$$\begin{aligned} \Pi_{ij}(q, i\Omega_n) = & \frac{T_n}{2m_f^2} \sum_{k, \sigma, \omega_n} (\mathbf{k} + \mathbf{q}/2)_i (\mathbf{k} + \mathbf{q}/2)_j \times \\ & \times G_{ff}(\mathbf{k} + \mathbf{q}, i\omega_n + i\Omega_n) G_{ff}(\mathbf{k}, i\omega_n) + \delta_{ij} \frac{\rho_f}{2m_f} \\ & + \frac{T}{2m_b^2} \sum_{k, \omega_n} (\mathbf{k} + \mathbf{q}/2)_i (\mathbf{k} + \mathbf{q}/2)_j \times G_b(\mathbf{k} + \mathbf{q}, i\omega_n \\ & + i\Omega_n) G_b(\mathbf{k}, i\omega_n) + \delta_{ij} \frac{n_b}{2m_b}. \end{aligned}$$

The vector field propagator has the form

$$D_{ij}^{-1}(q, i\Omega_n) = (\Pi_f + \Pi_b) (\delta_{ij} - q_i q_j / q^2), \quad (32)$$

where at the QCP and at $T=0$,

$$\begin{aligned} \Pi_f(q, i\Omega_n) = & \frac{N}{2m_f} \left[\frac{\pi |\Omega_n|}{v_F q} + (q/k_F)^2 \right], \\ \Pi_b(q, i\Omega_n) = & \frac{1}{2m_b} \left[\frac{\pi f_d |\Omega_n|}{q} + (q^2)/(2m_b) \right], \end{aligned} \quad (33)$$

with $f_d = \int (q^2/d) d^{d-1} q f_0(q) / (2\pi)^{d-1}$ and $f_0(q)$ is a UV cutoff.⁵⁰ The evaluation of Π_b is given in Eq. (D4). Pictorially, the polarization can be written as

When the bosons condense the gauge fields, propagators become massive. Note that the two-leg vertices in $\mathbf{a}_{\mu} - \mathbf{a}_{\nu}$ are

protecting the mass sector.⁵⁵ This is shown in Appendix F using again the Ward identity associated to the gauge invariance of the problem. It is checked as well in Appendix G by a direct evaluation at the first order.

VIII. ELIASHBERG THEORY

Our QCP corresponds to a $q=0$ transition. In Secs. VI and VII, we have treated the fluctuations within the RPA, for which the polarization is evaluated at the first loop order. A self-consistent treatment of the fluctuations is needed to control the results. Integrating the fermions out of the partition function is a dangerous uncontrolled step for such transitions. A better approach is the Eliashberg theory, controlled in a large N expansion. For the details, we refer the reader to the extensive review of this technique given in Ref. 18. For completeness, we recall here the reasoning and the main results. The Eliashberg theory relies on three steps. The first step is to neglect the renormalization of the vertices as well as the momentum dependence of the self-energy. In the second step, the Dyson equation is used to evaluate self-consistently the boson polarization and the fermion's self-energy. Then, one checks that the approximation is correct. Here, we have two types of fermions and two type of massless bosons as well—the order parameter and the vector gauge fields; the time gauge field a_0 being massive. The coupled Dyson equations are represented below with Feynman diagrams,

$$\begin{aligned} G_f^{-1}(k, \omega_n) &= i\omega_n - \epsilon_0 + i\Sigma_f(\omega_n), \\ G_c^{-1}(k, \omega_n) &= i\omega_n - \epsilon_k + i\Sigma_c(\omega_n), \\ D_b^{-1}(q, \Omega_n) &= \rho_0[-i\Omega_n + \delta + aq^2 + \Pi_{fc}(q, \Omega_n) - \Sigma_b(\Omega_n)], \\ D_{ij}^{-1}(q, \Omega_n) &= \rho_0[(q/k_F)^2 + \Pi_f(q, \Omega_n) + \Pi_b(q, \Omega_n)](\delta_{ij} \\ &\quad - q_i q_j / q^2), \end{aligned} \quad (34)$$

where

$$\Sigma_f(\omega_n) = \begin{array}{c} \begin{array}{c} b, a_\mu \\ \curvearrowright \\ \text{---} \cdot \text{---} \\ \text{f} \quad c \end{array} \end{array} ;$$

$$\Sigma_c(\omega_n) = \begin{array}{c} \begin{array}{c} b, a_\mu \\ \curvearrowright \\ \text{---} \cdot \text{---} \\ c \quad f \end{array} \end{array} ;$$

$$[\text{oooo}]^{-1} = [\text{~~~~}]^{-1} + [\text{~~~~}]^{-1};$$

$$\Sigma_b(\Omega_n) = \begin{array}{c} \begin{array}{c} a_\mu \\ \curvearrowright \\ \text{~~~~} \\ b \end{array} \end{array} ;$$

$$\Pi_{fc}(q, \Omega_n) = \begin{array}{c} \begin{array}{c} c \\ \curvearrowright \\ \text{---} \cdot \text{---} \\ b \quad f \end{array} \end{array} ;$$

$$\Pi_f(q, \Omega_n) = \begin{array}{c} \begin{array}{c} f \\ \curvearrowright \\ \text{---} \cdot \text{---} \\ a_\mu \quad a_\nu \\ f \end{array} \end{array} ;$$

$$\Pi_b(q, \Omega_n) = \begin{array}{c} \begin{array}{c} b \\ \curvearrowright \\ \text{~~~~} \\ a_\mu \quad a_\nu \\ b \end{array} \end{array} ;$$

Note that, in the above diagrams, the lines are full by construction, but the evaluation of the diagram does not change if the fermion propagators are taken to be bare. The bosonic “self-energy” Σ_b and the polarization Π_b are given in Appendix E.

The crucial point in the Eliashberg theory is to check if the three-leg vertices are small. We recall that, in the regime $T \geq E^*$, the dynamical exponent is $z=3$. This exponent characterizes as well the ferromagnetic QCP¹⁸ and the U(1) gauge theories,⁵¹ which have been studied in the literature. In both cases, the Eliashberg theory is controlled in the same way using the combined effects of the large N expansion and the curvature of the Fermi surface. We recall here the results.

There are two types of vertices depending on the incoming momentum and frequency. The static vertex,

$$\Gamma(0, 0) = \begin{array}{c} \begin{array}{c} \text{---} \cdot \text{---} \\ \curvearrowright \\ \text{---} \cdot \text{---} \\ \text{0}, 0 \quad k_F, 0 \end{array} \end{array}$$

obtained for vanishing incoming frequency, is small in the large N limit, going like $\Gamma(0, 0) \sim N^{-1/2}$. The dynamical vertex, however, obtained in the limit of nonvanishing, but still small frequency when $|\Omega_n| \ll v_F q$, is dangerous. Note that within our model, it is impossible to form the mixed fc vertex at the first order. Hence, we form it at the second order but evaluate each loop separately in Appendix B,

$$\Gamma(q, \Omega) = \begin{array}{c} \begin{array}{c} \text{---} \cdot \text{---} \\ \curvearrowright \\ \text{---} \cdot \text{---} \\ \text{0}, 0 \quad k_F, 0 \end{array} \end{array}$$

For bare fermion legs, it behaves as $\Gamma(q, \Omega_n) \sim \Omega_n^{(3-d)/3}$ [for

$d=3$, we get $\Gamma(q, \Omega_n) \sim -\Omega_n \log|\Omega_n|$, hence showing strong anomalies in the frequency dependence in the infrared sector. Fortunately, in the Eliashberg theory, the fermion legs are not bare but dressed with their proper self-energy. For $z=3$, the spinon and electron self-energy behave as $\Sigma(\omega_n) \sim |\omega_n|^{(d-3)/3}$ [with for $d=3$, $\Sigma(\omega_n) \sim -\omega_n \log|\Omega_n|$]. Dressing the fermion legs effectively kills the divergence in frequency. A subtle point is that, with a linearized Fermi surface, the resulting vertex is of order 1, with no small parameter. Including the curvature of the Fermi surface changes this situation. In the case where $q_y^2/m^* \gg v_f q_x$, where m^* is the curvature mass, we finally get $\Gamma(q, \Omega_n) \sim \beta^2 \log \beta^2$, with $\beta m^*/(Nm) \ll 1$. As we see, the justification of the Eliashberg theory in the case of a $z=3$, $q=0$ QCP is not simple; it requires both the presence of the curvature and an additional large N expansion (N being here the number of species of fermions), which is rather artificial. An additional caveat is that the large N limit cannot be rigorously taken since, if we did this, we would not include the diagrams corresponding to the fermionic self-energy, which scale like $N^{-1/3}$ in $D=2$, hence are subleading in the large N limit. The Eliashberg theory thus relies on a large N “expansion” rather than on a “large N limit.” This remark follows the similar observation made in Sec. VII, which the form of the boson propagator is not homogeneous in N .

Another regime of interest is the case where $z=2$ for intersecting Fermi surfaces. The theory is equivalent to the AF QCP whose Eliashberg spin fermion treatment is reviewed in Ref. 17. We refer the reader to this paper to get convinced of the smallness of the vertices.

The two regimes (ii) and (iii) of the boson propagator are not physically relevant since the boson propagator has only a small spectral weight in this regime compared to regime (iv). We still must check that the vertices are small. Let us check regime (ii) where the frequency part has a characteristic logarithmic-logarithmic dependence. In both two dimensions and three dimensions, we find that the static vertex scales like $\Gamma(0,0) \sim 1/N$. Curvature is needed to regularize the dynamical vertex, which goes like $\Gamma(q, \Omega_n) \sim (\Omega_n \log|\log|\Omega_n||)/\log|\Omega_n|$. Hence, large N is not needed for the smallness of the dynamical vertex in this regime. Details of the vertex calculation are given in Appendix B.

Last, the reader may wonder whether the analogous of the singularities discovered by Belitz–Kirkpatrick–Vojta (BKV)⁵⁶ exists in this theory. This issue lies beyond the Eliashberg theory but is of importance for the stability of $q=0$ QCPs. It has been shown by Belitz, Kirkpatrick, and Vojta⁵⁶ that singularities appear in the static sector, in the computation of the static, and temperature dependent polarization. Indeed, close to a $q=0$ QCP of ferromagnetic type, the static polarization,

$$\Pi(q, T) = \text{Diagram: A circular fermion loop with two external wavy lines labeled 'c'. The top and bottom arcs of the loop are labeled 'c'. A wavy line labeled 'S' enters from the left and another exits to the right. Arrows on the fermion lines indicate a clockwise direction.$$

vanishes at the first loop order. Technically, one can check

that, with zero incoming frequencies, poles of the fermion lines are in the same half-plane; hence, the static polarization vanishes at one loop. To get a nonzero result, one must include the first vertex correction.

In our case, it is worthwhile to notice first that the one-loop polarization has temperature dependence at lower energies due to the fact that we have two fermion species. Indeed, we find by direct computation an activated behavior in the case of gaped Fermi surfaces,

$$\Pi_{fc}(T) = N \frac{\rho_0}{(1-\alpha')} n_F \left[\frac{\alpha' v_F q^*}{(1-\alpha')} \right],$$

where n_F is the Fermi distribution function. This activated behavior is quite small. We have as well a source of damping coming from the gauge fields and leading to the temperature dependence (see Appendix E),

$$\Sigma_b(T) \sim T^{(d+2)/2}.$$

However, the BKV singularity comes from inserting vertices and self-energy (beyond Eliashberg theory) in the polarization bubble. It is dangerous because the first insertion leads to a contribution with *negative* sign, hence destabilizing the QCP. Here, we first observe that there is no first order vertex correction to the polarization Π_{fc} ; the diagram simply cannot be formed. At the first order, one has only self-energy insertions of the type

$$\Pi_{fc}^{(1)}(T) = \text{Diagram: Two diagrams showing a fermion loop with two external wavy lines labeled 'b'. The first diagram has a dashed line representing a self-energy insertion on the top arc. The second diagram has a solid line representing a self-energy insertion on the bottom arc. Arrows on the fermion lines indicate a clockwise direction.$$

We find, in the intermediate regime, in $D=3$

$$\Pi_{fc}^{(1)} \sim -N^{-2/3} T^{4/3}.$$

We argue that this contribution is smaller than E^* and can be neglected. In the low energy regime, we find that the mismatch between the two Fermi surfaces protects the system, independently of whether the Fermi surfaces intersect or not.

The first vertex correction comes at the two loop order as depicted below. Note that, contrarily to the nematic case,¹⁸ there is no cancellation between the vertices and self-energy insertions. This is due to the fact that we have two fermion species, hence the cancellation is spoiled, even though the transition is in the charge channel. We find that this correction behaves as

$$\Pi_{fc}^{(2)} \sim (N\alpha')^{-2/3} T^{5/3}$$

in the intermediate regime in $D=3$ and has a positive sign. It is thus not dangerous.

$$\Pi_{fc}^{(2)}(T) = \text{Diagram: A two-loop fermion diagram with two external wavy lines labeled 'b'. The diagram consists of two fermion loops connected by a wavy line. The top and bottom arcs of the loops are labeled 'c'. Arrows on the fermion lines indicate a clockwise direction.} \sim (N\alpha')^{-2/3} T^{5/3}$$

Note that the fermion lines are full in the computation of these diagrams. The interested reader can find more details about this discussion in Appendix C where we comment as well on $D=2$.

IX. IOFFE–LARKIN COMPOSITION RULES

In this section, we start the study of transport properties of this quantum critical gauge theory. A previous study exists,²⁴ but here we recast the formalism in terms of the Ioffe–Larkin composition rules for the resistivity and enlarge the discussion to the temperature dependence of the resistivity. It is known from the seminal paper of Ioffe and Larkin⁵⁷ that in the Coulomb phase of a gauge theory, both spinons and holons participate to transport and the total conductivity is constrained by the IL composition rules. In order to derive them for our model, we must expose the system to an external electromagnetic field \mathbf{A} . \mathbf{A} is attached to the conduction electrons and to the holons b .⁵⁸ The system is as well subjected to the internal fictitious gauge field \mathbf{a} [Eq. (27)]. \mathbf{a} is attached to the fields carrying the gauge charge, hence to the holon b and the spinon f_σ . We work in the Coulomb gauge, ensuring that $\nabla \cdot (\mathbf{A} + \mathbf{a}) = 0$. The system is invariant through

$$\begin{aligned} \mathbf{A} &\rightarrow \mathbf{A} + \nabla \theta_A, & \mathbf{a} &\rightarrow \mathbf{a} + \nabla \theta_a, \\ c &\rightarrow c \exp(i\theta_A) & f &\rightarrow f \exp(i\theta_a), \\ b &\rightarrow b \exp(i\theta_A - i\theta_a). \end{aligned} \quad (35)$$

In order to derive the IL composition rules, we expand the action for minimal coupling with the vector gauge fields. Note that the composition rules are completely general (see Appendix D); the expansion in minimal coupling is a matter of convenience,

$$\begin{aligned} S &= \int d\tau \sum_k f^\dagger G_f^{-1}(a_\mu) f + c^\dagger G_c^{-1}(A_\mu) c + b^\dagger D_b^{-1}(A_\mu, a_\mu) b, \\ &\simeq \int d\tau \sum_k [f^\dagger G_{0,f}^{-1} f + c^\dagger G_{0,c}^{-1} c + b^\dagger D_{0,b}^{-1} b + f^\dagger \mathbf{v}_f \cdot \mathbf{a} f \\ &\quad + c^\dagger \mathbf{v}_c \cdot \mathbf{A} c + b^\dagger \mathbf{v}_b \cdot (\mathbf{a} + \mathbf{A}) b], \end{aligned} \quad (36)$$

where the vertices \mathbf{v}_f , \mathbf{v}_c , and \mathbf{v}_b are determined from the expansion of the effective Lagrangian to the first order in \mathbf{a} , \mathbf{A} .⁵⁹ After integrating out the matter fields f , c , and b , the effective action for minimal coupling to the gauge fields reads

$$\begin{aligned} S\{A, a\} &= \frac{T}{2} \int \frac{d^d k}{(2\pi)^d} \sum_{\omega_n} [\mathbf{A}_\alpha(\omega, k) \Pi_c^{\alpha\beta}(\omega, k) \mathbf{A}_\beta \\ &\quad + (\mathbf{A}_\alpha - \mathbf{a}_\alpha) \Pi_b^{\alpha\beta}(\omega, k) (\mathbf{A}_\beta - \mathbf{a}_\beta) \\ &\quad + \mathbf{a}_\alpha(\omega, k) \Pi_f^{\alpha\beta}(\omega, k) \mathbf{a}_\beta]. \end{aligned} \quad (37)$$

The polarization bubble $\Pi(\omega, k)$ can be decomposed into its longitudinal and transverse parts,

$$\Pi_{\alpha\beta} = \left(\delta_{\alpha\beta} - \frac{k_\alpha k_\beta}{k^2} \right) \Pi_1 + \frac{k_\alpha k_\beta}{k^2} \Pi_2. \quad (38)$$

Following IL, we integrate over the fictitious gauge field \mathbf{a} in Eq. (2) to get the effective action for the external electric field,

$$S\{A, a\} = \frac{T}{2} \int dk \sum_\omega \mathbf{A}_\alpha(\omega, k) [\Pi_c + (\Pi_b^{-1} + \Pi_f^{-1})^{-1}] \mathbf{A}_\beta. \quad (39)$$

Hence, the total polarizability of the system is

$$P_1 = \Pi_c + (\Pi_f^{-1} + \Pi_b^{-1})^{-1}. \quad (40)$$

Using the Kubo formula

$$\sigma = \frac{i\Pi(\omega)}{\omega}, \quad (41)$$

we get for the conductivity

$$\sigma = \sigma_c + (\sigma_f^{-1} + \sigma_b^{-1})^{-1}. \quad (42)$$

Note that the composition rule for the conductivity can be derived in a simpler way using solely the constraint attached to the gauge symmetry; this calculation is given in Appendix D. The composition rules [Eq. (40)] are powerful enough to allow a complete discussion of the electrical transport close to the QCP. One observes that the holons are “sandwiched” between the spinons and the conduction electrons. If Π_b^{-1} dominates Π_f^{-1} , then it is very unlikely that Π_b will dominate Π_c since Π_c already dominates Π_f . Hence, we infer from the simple form of Eq. (40) that Π_c is the most important part. The transport is dominated the conduction electrons.

Let us first examine the limit of zero temperature. On the heavy Fermi liquid side, the holons b are perfect conductors and the spinons are massless fermions so that

$$\Pi_b = \frac{n_b e^2}{m_b}, \quad \Pi_f = \frac{n_f e^2}{m_f} \frac{-i\omega\tau_f}{(1 - i\omega\tau_f)}, \quad (43)$$

where we have used a Drude formula⁶⁰ for the polarization of the f spinons and τ_f is the scattering lifetime of the spinons,⁶¹ which writes $\tau_f^{-1} \sim \tau_0^{-1} + T^2$ in the heavy Fermi liquid. Note that we have taken into account the effect of impurities in the scattering time of the spinons. This corresponds to dressing the spinon lines with disorder, but neglecting the vertex corrections. In the limit of low frequencies, $\Pi_b^{-1} + \Pi_f^{-1}$ is fully dominated by the second term; hence, the holons do not affect the residual conductivity. We get, on the heavy Fermi liquid side and in the limit of low frequencies,

$$\Pi_1 \simeq \Pi_c + \Pi_f, \quad (44)$$

with

$$\Pi_c = \frac{n_c e^2}{m_c} \frac{-i\omega\tau_c}{(1 - i\omega\tau_c)}. \quad (45)$$

In Eq. (44), the effect of impurities is implicitly taken into account in the scattering lifetime of the conduction electrons $\tau_c^{-1} \sim \tau_0^{-1} + T^2$. In the limit of zero frequencies, we get

$$\sigma_1 = \frac{n_c e^2 \tau_c}{m_c} + \frac{n_f e^2 \tau_f}{m_f}, \quad (46)$$

while, on the localized side of the transition, only the conduction electron conducts. The residual conductivity thus jumps at the transition; on the heavy Fermi liquid side, the f

spinon starts abruptly to conduct. This result is in agreement with the study of Ref. 24. Note, however, that the jump in the conductivity obtained in this model is very unlikely to be detectable, since $m_c \ll m_f$.⁶¹

We turn next to the temperature dependence of the conductivity at the QCP. We first focus on the low temperature regime, already studied in Ref. 23, saving the study of the intermediate temperature regime for Sec. X. As in Sec. VIII, there are two cases of interest. In case (a), there is a gap in the continuum of the particle-hole excitations. Because of the gap, the electron and spinon lifetime are not affected by the scattering with the holons, and we get the standard Landau–Fermi liquid law, $\tau_f^{-1} \sim \tau_c^{-1} \sim \tau_0^{-1} + T^2$. The damping of the holons does not come from the particle-hole continuum but only from the gauge fields Σ_b . This damping of the holons itself produces a finite bosonic lifetime. The polarization writes (see Appendix E)

$$\Pi_b = \frac{e^2}{m_b} (-i\omega\tau_b), \quad (47)$$

with

$$\begin{aligned} \tau_b &\sim -\log T \quad \text{in } D=2, \\ \tau_b &\sim T^{5/4} \quad \text{in } D=3. \end{aligned} \quad (48)$$

One sees that, in that case as well, the sum $\Pi_f^{-1} + \Pi_b^{-1}$ is dominated by Π_b^{-1} for $D=2$ and by Π_f^{-1} for $D=3$. Nevertheless, in both cases, the conductivity is dominated by the conduction electrons as can be seen from Eq. (40). The resistivity thus varies like T^2 at the QCP,

$$\rho \sim \rho_0 + T^2 \quad \text{in } D=3. \quad (49)$$

This result contradicts the previous study.²³ In our view, the contribution of the conduction electrons to the conductivity was overlooked in Ref. 23.

The second case of interest is when the two Fermi surfaces intersect, called case (b). Here, the particle-hole continuum has no gap, hence the bosons are not perfect conductors anymore but are damped by the particle-hole continuum. We write (see Appendix E)

$$\Pi_b = \frac{e^2}{m_b} (-i\omega\tau_b), \quad (50)$$

where τ_b carries the temperature dependence of the polarization. We find for $z=2$

$$\begin{aligned} \tau_b &\sim -\log T \quad \text{in } D=2, \\ \tau_b &\sim \sqrt{T} \quad \text{in } D=3. \end{aligned} \quad (51)$$

Now in the Eliashberg theory, damping from the gauge fields leads to $\tau_f^{-1} \sim \tau_0^{-1} + \Sigma_f(T)$ with

$$\Sigma_f(T) \sim \begin{cases} T^{2/3} & \text{for } D=2 \\ -T \log T & \text{for } D=3. \end{cases}$$

One sees that, in that case as well, the sum $\Pi_f^{-1} + \Pi_b^{-1}$ is dominated by Π_b^{-1} for $D=2$ and by Π_f^{-1} for $D=3$. Nevertheless, in both cases, the conductivity is dominated by the con-

duction electrons. Since the regime is characterized by $z=2$, the conduction electrons have the inverse scattering lifetime $\Sigma_c \simeq T^{3/2}$ in $D=3$. Since the backscattering processes are naturally present in the model (see Sec. X), this regime is equivalent to the AF SDW scenario, with

$$\rho \sim \rho_0 + T^{3/2} \quad \text{in } D=3. \quad (52)$$

A last remark for this section is that we recover the result of Ref. 24 that although the gauge fields are gapped in the Higgs phase, the external electromagnetic field is not, which prohibits—thank goodness—Meissner effect in the heavy Fermi liquid phase. The easiest way to see it is to make the change in variable $a'_\mu = a_\mu + A_\mu$ in Eq. (36). The fictitious gauge fields are now a'_μ and the external gauge fields are decoupled from the holons,

$$S_{\text{int}} = b^\dagger \mathbf{v}_b \cdot \mathbf{a}' b + c^\dagger \mathbf{v}_c \cdot \mathbf{A} c + f^\dagger \mathbf{v}_f \cdot (\mathbf{a}' - \mathbf{A}) f. \quad (53)$$

One now follows Appendix F and writes the Ward identity related to the *external* gauge field. Since the source terms can be set to zero (only the holons get a nonvanishing source term), the mass of the electromagnetic field vanishes like

$$-iq^\mu \Pi_{A_\mu A_\nu} = 0. \quad (54)$$

X. QUASILINEAR RESISTIVITY

We examine here the transport in the intermediate regime. This regime differs from the low temperature one by its dynamical exponent which is now $z=3$. In this regime, the IL composition rules are still valid, with

$$\begin{aligned} \tau_b &\sim -\log T \quad \text{for } D=2, \\ \tau_b &\sim T^{1/3} \quad \text{for } D=3, \end{aligned} \quad (55)$$

hence the holons still do not participate to the transport. As before, the conductivity is dominated by the conduction electrons. In this section, we examine in more detail the Drude form assumed in Eq. (44). The arguments have been given in a previous work, and we recall them here for clarity.²⁷ The main idea is that the Drude form is valid, with the scattering lifetime of the conduction electrons given by

$$\tau_c^{-1} \sim -T \log T \quad (56)$$

in $D=3$. Equation (56) is the typical scattering lifetime for a $z=3$ QCP, such as, for example, a ferromagnet. The important question is “how does the current decay in this special $q=0$ phase transition.” The unique feature of this QCP is that the current naturally decays through the lattice of f electrons. Contrarily to a usual ferromagnetic QCP or nematic QCP where translational invariance is not broken at the phase transition, here translational invariance is naturally broken since the f electrons are on the brink of localization. Hence, there is no need for external translation invariance breakers, such as impurities, to break translational invariance. Umklapp processes are naturally present, which decay the current. In this sense,

$$\tau_{\text{tr}} \approx \tau_{\text{QP}}, \quad (57)$$

where τ_{tr} is the transport time, while τ_{QP} is the quasiparticle lifetime. For $z=3$, $D=3$, it has the standard form

$$\tau_{\text{QP}}^{-1} \sim T. \quad (58)$$

Our claim is that the electric transport in this phase is correctly described by the Drude polarization

where here we have used bare lines. More precisely, using the Kubo formalism, one can first show that the conduction electron polarization is unaffected by coupling to the bosons and the f fermions. The coupling to f and b is protected by gauge invariance. Pictorially, we mean that

This comes from the fact that $[\Pi]^{-1} = \Pi_f + \Pi_b$. The next observation is that the vertex corrections are negligible in this regime; namely, the next leading order to the Drude formulas is of order $(\alpha')^2$ and $1/N$, as shown in the diagram below,

Hence, in this regime, the transport is simple and electrical conductivity can be expressed through the simple Drude formulas. The evaluation of the inverse scattering time in $D=3$ is given in Appendix H. We get

$$\begin{aligned} \tau_{\text{tr}} &\sim T \log(T/E^*) \text{ in } D=3, \\ \tau_{\text{tr}} &\sim T^{2/3} \text{ in } D=2. \end{aligned} \quad (59)$$

Note that the logarithm in $D=3$ has a thermal origin; it differs from the logarithm which appears in the real part of the self-energy in $D=3$.

XI. SUMMARY OF THERMODYNAMIC AND TRANSPORT

To summarize transport and thermodynamics close to the QCP, we distinguish regime I for $T \leq E^*$ and regime II for

TABLE I. Transport and thermodynamic exponents in the low temperature regime when the particle-hole continuum is gapped.

$T \leq E^*$ (Regime I)	C_v	$\Delta\rho(T)$	$\chi(T)$
$D=3$	$-T \log(T)$	T^2	χ_0
$D=2$	$T^{2/3}$	T^2	χ_0

$T \geq E^*$. The exponents for transport and thermodynamics in regime I depend on the form of the spinon Fermi surface. If there is a gap between the spinon and electron Fermi surfaces, as shown in Fig. 3 for case (a), then the anomalous exponents for the effective mass—appearing in C_v —are due to the massless gauge fields with $z=3$. The electrical resistivity is dominated by the conduction electrons, and since the scattering with the spinons is gapped, it follows the usual T^2 law characteristic of the Landau–Fermi liquid. The susceptibility does not couple directly to the critical modes, hence here again the Fermi liquid law is recovered. The exponents are summarized in Table I.

We see that the situation is peculiar in the sense that the Landau–Fermi liquid paradigm is broken for the thermodynamics only. The resistivity behaves as T^2 even though the residual resistivity jumps at the Fermi surface. There is no trace of anomalous exponents for the dynamic spin susceptibility, a fact which poorly fits the experimental observations.

The second case is when $T \leq E^*$, but the spinon and electron Fermi surfaces intersect. We call this regime I'. In that case, the particle-hole continuum goes down to $T=0$ with hot regions at the intersection of the two Fermi surfaces. The situation is analogous to the AF SDW QCP, except that the critical modes are solely in the charge channel. The results are summarized in Table II.

In our view, the most interesting regime is for $T \geq E^*$. In that case, the exponents do not depend on the shape of the spinon Fermi surface, but the very existence of this regime requires the presence of a spinon Fermi surface at the QCP. Here, the transport is simpler than closer to the QCP. The resistivity shows a quasilinear behavior in $D=3$ and a sub-linear exponent in $D=2$. The results are summarized in Table III. Note that the temperature dependence of the spin susceptibility, although departing from the standard Landau–Fermi liquid law, still does not show anomalous exponents.

XII. CONCLUSIONS

In this paper, we have given the simplest consistent treatment of a selective Mott transition in the Anderson lattice

TABLE II. Transport and thermodynamic exponents in the low temperature regime, where the spinon and electron Fermi surfaces intersect.

$T \leq E^*$ (Regime I')	C_v	$\Delta\rho(T)$	$\chi(T)$
$D=3$	$-T \log(T)$	$T^{3/2}$	χ_0
$D=2$	$T^{2/3}$	$-T \log T$	χ_0

TABLE III. Transport and thermodynamic exponents in the marginal Fermi liquid regime around the Kondo breakdown QCP. The exponents are in agreement with those of Ref. 27.

$T \gg E^*$ (Regime II)	C_v	$\Delta\rho(T)$	$\chi(T)$
$D=3$	$T \log(T/E^*)$	$T \log(T/E^*)$	$T^{4/3}$
$D=2$	$T^{2/3}$	$T^{2/3}$	$-T \log(T)$

using a U(1) slave-boson technique associated with an Eliashberg treatment of the vertices. We find that the QCP exists and has a multiscale character. At the QCP below E^* , the exponents for thermodynamics and transport depend on the shape of the spinon and electron Fermi surfaces. When the particle-hole continuum is gapped, the anomalous transport scattering is gapped as well, and the resistivity follows the Landau–Fermi liquid law.^{62,63} The effective mass is dominated by the fluctuations of the transverse gauge fields showing a Reizer singularity.⁵⁴ If the spinon and electron Fermi surfaces intersect, the particle-hole continuum is gapless and the transport and thermodynamics are anomalous down to the lowest temperature, with $z=2$ for $T \leq E^*$. Above the energy scale E^* , the resistivity does not depend on the shape of the spinon Fermi surface, and we get a universal quasilinear resistivity in $D=3$. In our view, the important question raised by our study is the question of the presence or not of a selective Mott transition in the Anderson lattice. Said in general words, one can reasonably ask whether we believe that the anomalous properties observed in heavy fermions are due to a Mott localization of the f electrons. If we believe that it is the right answer, then the U(1) slave-boson gauge theory is the most straightforward approach to such a phenomenon. It would be very interesting to have studies from other techniques, such as DMFT, to first confirm the presence of the transition and, if it there, to give more details about the elementary excitations.

It is reasonable to ask whether the U(1) slave-boson theory, although being the simplest description of the Mott transition, is the appropriated tool. This question is of relevance as well for the cuprate superconductors, where gauge theories, with sometimes bigger algebra like SU(2), have been extensively used to describe the approach to the Mott state.^{42,45} It is clear from the above study that this approach suffers from what we would call spinology. Fermionic spinons with a finite Fermi surface are needed at the QCP for the QCP to exist at all. One can reasonably question this feature and wonder whether under more powerful techniques, this feature would survive. Nevertheless, before discarding the U(1) slave-boson gauge theory for the Anderson lattice, one must consider that it gives a very interesting regime with a quasilinear scattering and transport lifetime in 3D. This unique feature is not easily obtained within any theory and the good point is that it does not depend on the shape of the spinon Fermi surface, but only on its presence at the QCP—hence, it is a direct consequence of the “fractionalization” of the heavy electron at the QCP. We can use this regime for making experimentally testable predictions. A first application to He³ bilayers has been performed.³¹ We

can as well make predictions for the thermal transport in this regime and call for experimental confirmation or invalidation.

ACKNOWLEDGMENTS

I am indebted to M. Norman and I. Paul for countless discussions on the similar Kondo–Heisenberg model. Many ideas of this paper came from interactions with them, related to this previous study. The description of the quasilinear resistivity benefited from a useful discussion with D. L. Maslov and the study of the Ward identities and the Ioffe–Larkin composition rule, from useful interactions with K.-S. Kim and O. Parcollet, and a very useful, heated discussion with P. Coleman. A special thank to C. Bena and A. V. Chubukov for a useful reading of the paper. This work is supported by the French National under Grant No. ANR36ECCEZZZ.

APPENDIX A: EVALUATION OF THE INTEGRALS FOR THE MEAN-FIELD

At $T=0$, the calculation of the integrals used in the mean-field treatment is analytical for linearized bands: We call

$$\mathcal{A} = T \sum_{k, \sigma, \omega_n} G_{ff}(k, i\omega_n),$$

$$\mathcal{B} = T \sum_{k, \sigma, \omega_n} G_{fc}(k, i\omega_n)/(bV + \sigma_0),$$

$$\mathcal{C} = T \sum_{k, \sigma, \omega_n} \epsilon_k G_{ff}(k, i\omega_n).$$

We diagonalize the 2×2 matrix¹⁰ which accounts for the hybridization of the f and c bands,

$$X_1 = \frac{1}{2}[\epsilon_k^0 + \epsilon_k - \sqrt{\Delta}],$$

$$X_2 = \frac{1}{2}[\epsilon_k^0 + \epsilon_k + \sqrt{\Delta}],$$

$$\Delta = (\epsilon_k^0 - \epsilon_k)^2 + 4(\sigma_0 + bV)^2.$$

The integrals are all performed in the same way, first by summing over the Matsubara frequencies and second by doing the momentum integration. The momentum integration is done by linearization of the band,

$$\begin{aligned} \mathcal{A} &= NT \sum_{k, \omega_n} \frac{(i\omega_n - \epsilon_k)}{(i\omega_n - X_1)(i\omega_n - X_2)} \\ &= N\rho_0 \int_{-D}^D d\epsilon \int \frac{-n_F(z)}{2i\pi} \frac{(z - \epsilon)}{(z - X_1)(z - X_2)} dz, \end{aligned}$$

where the contour is on the whole complex plane,

$$\begin{aligned}
&= N\rho_0 \int_{-D}^D d\epsilon \left(\frac{n_F(X_1)(X_1 - \epsilon_k)}{(X_1 - X_2)} - \frac{n_F(X_2)(X_2 - \epsilon_k)}{(X_1 - X_2)} \right) \\
&= \frac{N\rho_0}{2} \int_{-D}^{\epsilon_m} d\epsilon \frac{-y + \sqrt{y^2 + 4(bV + \sigma_0)^2}}{\sqrt{y^2 + 4(bV + \sigma_0)^2}} \\
&\quad - \frac{N\rho_0}{2} \int_{-D}^{\epsilon_p} d\epsilon \frac{-y - \sqrt{y^2 + 4(bV + \sigma_0)^2}}{\sqrt{y^2 + 4(bV + \sigma_0)^2}},
\end{aligned}$$

with ϵ_m and ϵ_p as the Fermi levels for the upper and lower bands, respectively.

$$\epsilon_m = (-\epsilon_f + \alpha' \mu - \sqrt{(\epsilon_f + \alpha' \mu)^2 + 4\alpha'(bV + \sigma_0)^2}) / (2\alpha'),$$

$$\epsilon_p = (-\epsilon_f + \alpha' \mu + \sqrt{(\epsilon_f + \alpha' \mu)^2 + 4\alpha'(bV + \sigma_0)^2}) / (2\alpha'),$$

with the conditions

$$-D \leq \epsilon_m \leq 0, \quad 0 \leq \epsilon_p \leq D,$$

and

$$\alpha' = \alpha b^2 + \phi_0 / D.$$

One obtains

$$\begin{aligned}
\mathcal{A} &= \frac{N\rho_0}{2(1 - \alpha')} (-2y_{-D} + y_m - \sqrt{y_m^2 + 4(bV + \sigma_0)^2} + y_p \\
&\quad + \sqrt{y_p^2 + 4(bV + \sigma_0)^2}),
\end{aligned}$$

$$y_m = (1 - \alpha')\epsilon_m - \epsilon_f - \mu,$$

where

$$y_p = (1 - \alpha')\epsilon_p - \epsilon_f - \mu,$$

$$y_{-D} = -(1 - \alpha')D - \epsilon_f - \mu.$$

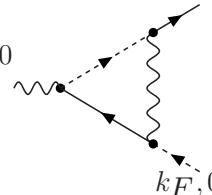
We proceed in the same way for \mathcal{B} and \mathcal{C} to find

$$\mathcal{B} = \frac{N\rho_0}{(1 - \alpha')} \log \left[\frac{y_m + \sqrt{y_m^2 + 4(bV + \sigma_0)^2}}{y_p + \sqrt{y_p^2 + 4(bV + \sigma_0)^2}} \right],$$

$$\begin{aligned}
\mathcal{C} &= \frac{N\rho_0}{2(1 - \alpha')^2} \left[-2(\epsilon_f + \mu)(y_{-D}) + y_{-D}^2 + 2(bV + \sigma_0)^2 \right. \\
&\quad \times \log \left(\frac{y_m + \sqrt{y_m^2 + 4(bV + \sigma_0)^2}}{y_p + \sqrt{y_p^2 + 4(bV + \sigma_0)^2}} \right) + (\epsilon_f + \mu)y_m + y_m^2 \\
&\quad - (y_m/2 + \epsilon_f + \mu)\sqrt{y_m^2 + 4(bV + \sigma_0)^2} + (\epsilon_f + \mu)y_p + y_p^2 \\
&\quad \left. - (y_p/2 + \epsilon_f + \mu)\sqrt{y_p^2 + 4(bV + \sigma_0)^2} \right].
\end{aligned}$$

APPENDIX B: EVALUATION OF THE INTEGRALS FOR THE VERTICES

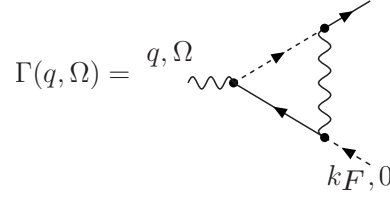
In this appendix, we focus on the evaluation of the vertices for regime II where we have logarithmic frequency dependence of the polarization. We call $\bar{g} = V^2 \rho_0$ with V as the coupling constant between the soft modes and the f and c electrons and ρ_0 as the density of states of the c electrons. Note that although it is not possible to form the vertex correction at the first loop, we still evaluate the fictitious one-loop vertex below, knowing that the two-loop vertices behave as products of the one-loop ones. We start with the static vertex

$$\Gamma(0,0) = 0,0$$


$$\begin{aligned}
\Gamma(0,0) &= \frac{\bar{g}}{-N \log(\alpha')} \int \frac{d^d q d\omega}{(2\pi)^{d+1}} \frac{1}{q^2 - a \log|\omega_n|} \frac{1}{(i\omega_n + \alpha' v_{Fq} \cos \theta)(i\omega_n - v_{Fq} \cos \theta)}, \\
&= \frac{\bar{g}}{N \log(\alpha')(1 - \alpha')} \int \frac{q^2 dq d\omega}{(2\pi)^3} \frac{1}{-i\omega_n(q^2 + a \log|\omega_n|)} \left(\frac{-1}{v_{Fq}} \right) \log \left[\frac{v_{Fq} - x}{\alpha' v_{Fq} - x} \right]_{x=-1}^{x=1} = \frac{\bar{g}(-\log \alpha)}{N(1 - \alpha')12(2\pi)^2 E_F},
\end{aligned}$$

with $a = 1/\log(\alpha')$. Hence, the static vertex is small in $1/N$.

We next evaluate the dynamical vertex, with linearized Fermi surfaces



$$\begin{aligned}\Gamma(q, \Omega) &= \frac{\bar{g}}{-N \log(\alpha')} \int \frac{d^d q d\omega}{(2\pi)^{d+1}} \frac{1}{q^2 - a \log|\omega_n|} \frac{1}{(i\omega_n + \alpha' v_F q \cos \theta)(i\omega_n + i\Omega_n - v_F q \cos \theta - v_F Q_x)}, \\ &= \frac{\bar{g}}{-N \log(\alpha')(2\pi)^3} \frac{i}{i\Omega_n - v_F Q_x} \int_{-\Omega_n}^0 d\omega \log \frac{(-\log \alpha')}{\log |\omega_n|}, \\ &\simeq \frac{\bar{g}}{-N \log(\alpha')(2\pi)^3} \times \frac{i}{i\Omega_n - v_F Q_x} [\Omega_n \log \log |\Omega_n| - \text{Li}(-\Omega_n)].\end{aligned}\quad (\text{B2})$$

We see from Eq. (B1) that for $Q_x=0$, the vertex has a log log singularity. It is not small.

The same evaluation with the curvature of the Fermi surface gives

$$\begin{aligned}\Gamma(q, \Omega_n) &= \frac{\bar{g}}{-N \log(\alpha')} \int \frac{d^d q d\omega}{(2\pi)^{d+1}} \frac{1}{q^2 - a \log|\omega_n|} \frac{1}{[i\omega_n - \alpha' v_F q \cos \theta - \alpha' q_\perp^2/(2m)]} \frac{1}{[i\omega_n + i\Omega_n - v_F q \cos \theta - v_F Q_x - q_\perp^2/(2m)]}, \\ &= \frac{\bar{g}}{-N \log(\alpha')2(2\pi)^3} \int_{-\Omega_n}^0 (-i d\omega) \frac{1}{[Q_x v_F + (1 - \alpha') \log|\omega_n|/\log \alpha']} \log \left(\frac{-\log \alpha'}{\log |\omega_n|} \right) \\ &\simeq \frac{\bar{g}}{-N \log(\alpha')2(2\pi)^3} \frac{i\Omega_n \log(-\log |\Omega_n|)}{(1 - \alpha' \log |\Omega_n|/\log \alpha')}\end{aligned}$$

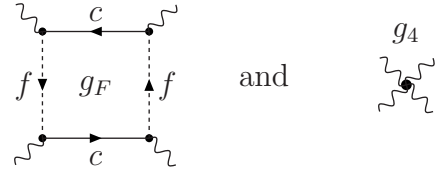
We see now that the curvature regularizes the vertex both in large N and in the infrared frequency sector.

APPENDIX C: INSTABILITIES BEYOND THE ELIASHBERG THEORY

In this section, we evaluate diagrams beyond Eliashberg theory, but those are potentially dangerous for the static sector of any $q=0$ QCP. As mentioned in the main text, such singularities were discovered by BKV⁵⁶ and are typical of the type of problems coming from the presence of a finite Fermi surface in the theory. Precisely, we want to evaluate

$$\Pi_{fc}^{(1)}(T) = \Pi_a^{(1)} + \Pi_b^{(1)}$$

We first note that the two diagrams are proportional, $\Pi_a^{(1)} = \alpha' \Pi_b^{(1)}$, and that there is no corresponding vertex insertion at the first order. One can check that, in the low energy regime $T \leq E^*$, the two diagrams are not singular, since the average gap between the spinon and electron Fermi surfaces protects it. Here, we want to check the stability in the intermediate regime for $T \geq E^*$. We have $z=3$ in the boson propagator. To understand the source of the problem, it is instructive to compare the following four-field diagrams,



where g_4 is a mode-mode coupling constant, coming, for example, from the term $-J_0 n_i n_j/4$ in Eq. (3). The g_4 mode-mode coupling is standard in a ϕ^4 theory and provides correction to scaling extensively studied in, for example, chapter 42 of Ref. 64. If $g_4 \geq 0$, the ϕ^4 theory is stable and, close to a QCP, the corrections to scaling follow the law

$$m_b(T) = \text{diagram} \sim T^{(d+z-2)/z}$$

One sees that, in a fermionic theory, one can form corrections to scaling from the fermion vertex g_F which leads to our two diagrams, $\Pi_a^{(1)}$ and $\Pi_b^{(1)}$. The difference between g_F and g_4 is that the fermion loop is dangerous and can change the sign of the vertex. According to the value of z , it can as well lead to a more relevant term than the standard ϕ^4 corrections to scaling.

We turn to the computation of the diagrams. With $\bar{g} = 8k_F^2 V^2 / \rho_0$ and $c = \rho_0 N / (\alpha' v_F)$.

$$\begin{aligned} \Pi_a^{(1)}(T) = N\bar{g}\rho_0 T \sum_{n,m \neq 0} \int \frac{d^d q}{(2\pi)^d} d\epsilon_k D_b(q, \Omega_m) G_c^2(k, \omega_n) G_f(k, \omega_n) G_f(k+q, \omega_n + \Omega_m) = N\rho_0 \bar{g} T \sum_{n,m} \int \frac{d^d q}{(2\pi)^d} d\epsilon_k \frac{1}{c|\Omega_m|/q + aq^2} \\ \times \frac{1}{[i\omega_n + i\Sigma_c(\omega_n) - \epsilon_k + \mu]^2} \frac{1}{[i\omega_n + i\Sigma_f(\omega_n) - \alpha' \epsilon_k - \epsilon_f]} \frac{1}{[i\omega_n + i\Omega_m + i\Sigma_f(\omega_n) + i\Sigma_f(\Omega_m) - \alpha' \epsilon_k - \alpha' v_F q_x - \epsilon_f]}. \end{aligned}$$

We have $\text{sgn}[\Sigma_{f,c}(\omega_n)] = \text{sgn}[\omega_n]$. We perform first the integration over ϵ_k , noticing that the integral is nonzero if the poles are in the same half-plane. To fix the ideas, we take $\omega_n < 0$ while $\omega_n + \Omega_m > 0$ (the result is identical to the other choice). We then close the contour in the upper half-plane to catch the pole coming from the last factor. We obtain, after neglecting the terms proportional to α' and neglecting $i\omega_n$ compared to $i\Sigma_{f,c}(\omega_n)$ in the Green's functions,

$$\Pi_a^{(1)}(T) = N\alpha' \bar{g}\rho_0 T \sum_{m \neq 0, -m \leq n \leq 0} \int \frac{d^d q}{(2\pi)^d} \frac{1}{c|\Omega_m|/q + aq^2} \frac{2i\pi}{[i\Sigma_f(\Omega_m) - \alpha' v_F q_x]} \frac{1}{[i\Sigma_f(\Omega_m) + i\Sigma_f(\omega_n) - \alpha' v_F q_x - \epsilon_f]^2}.$$

Keeping only the dependence in Ω_n in the integrand, we get

$$= N\alpha' \bar{g}\rho_0 T \sum_m \int \frac{d^d q}{(2\pi)^d} \frac{i\Omega_m}{c|\Omega_m|/q + aq^2} \frac{1}{[i\Sigma_f(\Omega_m) - \alpha' v_F q_x]^3}. \quad (C1)$$

The calculation in $D=2$ and $D=3$ differs at this point.

1. $D=3$

Since there is only one pole in the last factor, the integration over q_x lead to a typical q_x of the order of Σ_f (it is the reason why full fermion lines can be safely replaced by bare ones in the Eliashberg theory). One possibility is that the integration over q_x does not vanish due to the branch cut in the boson propagator $q_x \sim q_\perp \sim |\Omega_m|^{1/3}$. It is what happens in $D=3$. We find

$$\Pi_a^{(1)}(T) \simeq -T^{4/3}. \quad (C2)$$

Note that the minus sign is of importance. We argue though, that since we are in the intermediate regime where $T \gg E^*$, the correction in $T^{4/3}$ is irrelevant, just giving an extra UV cutoff for the intermediate regime. The stability of this regime is thus ensured in $D=3$.

2. $D=2$

In $D=2$, the situation is more complex. The branch cut at $q_x \sim q_\perp \sim |\Omega_m|^{1/3}$ would lead to $\Pi_a^{(1)}(T) \simeq -T$, but there is a stronger singularity first discovered in Ref. 18. Indeed, we suppose $q_y \gg q_x$ and expand $q = \sqrt{q_x^2 + q_y^2} \simeq |q_y| + q_x^2/(2|q_y|)$. We find

$$\begin{aligned} \Pi_a^{(1)}(T) = N \frac{\alpha' \bar{g}\rho_0}{(2\pi)^2} T \sum_{m \neq 0} \int_{|q_x|}^{\Lambda} dq_y \frac{i\Omega_m}{c|\Omega_m|} \int dq_x [|q_y| \\ + \frac{q_x^2}{2|q_y|}] \frac{1}{[i\Sigma_f(\Omega_m) - \alpha' v_F q_x]^3}, \end{aligned}$$

as the integration over q_y now leads to a logarithmic singularity in q_x ,

$$I_{\text{sing}} = \int dq_x \frac{q_x^2 \log(\Lambda/|q_x|)}{[i\Sigma_f(\Omega_m) - \alpha' v_F q_x]^3}.$$

I_{sing} is performed by continuation in the upper half-plane if $\Omega_m \leq 0$ and in the lower half-plane if $\Omega_m \geq 0$ so that to avoid the pole in the Green's function. Changing variables in $q_x = iz$, we get

$$\begin{aligned} I_{\text{sing}} = - \int_0^{\Lambda} idz \text{sgn}(\Omega_m) \frac{(-iz)^2 [\log(-iz) - \log(iz)]}{(-i)^3 [|\Sigma_f(\Omega_m)| + \alpha' v_F z]^3}, \\ = \frac{-i\pi \text{sgn}(\Omega_m)}{(\alpha' v_F)^3} \log\left(\frac{\Lambda}{|\Sigma_f(\Omega_m)|}\right). \end{aligned}$$

Setting things together, we get

$$\Pi_a^{(1)}(T) = N \frac{\alpha' \bar{g}\rho_0}{(2\pi)^2} T \sum_{m \neq 0} \frac{i\Omega_m - i\pi \text{sgn}(\Omega_m)}{c|\Omega_m| (\alpha' v_F)^3} \log\left(\frac{\Lambda}{|\Sigma_f(\Omega_m)|}\right),$$

since $T \Sigma_{-N/T}^{\Lambda/T} = Cst$, we find that the T dependence of the above comes from the $m=0$ term only. Finally,

$$\Pi_a^{(1)}(T) = - \frac{\alpha' \bar{g}\rho_0}{(2\pi)^2} \frac{\pi}{c(\alpha' v_F)^3} T \log\left(\frac{\Lambda}{T}\right). \quad (C3)$$

This result sets the intermediate regime in a fragile situation. This term is of negative sign and dominant compare to E^* ; it has the potential to destabilize the regime. Note that in $D=2$, corrections to scaling coming from the g_4 interactions have the same temperature dependence ($-T \log T$) but with a positive sign. Corrections to scaling hence compete with $\Pi_a^{(1)}$ and tend to stabilize the fixed point. We have reached here the limit of the Eliashberg theory. Whether the intermediate regime is stable or not in $D=2$ depends on whether we have strong enough corrections to scaling of positive sign. This requires, for example, strong enough ferromagnetic short range fluctuations [$J_0 < 0$ in Eq. (3)]. The stability of the intermediate regime is a matter of prefactors between the two terms.

APPENDIX D: IOFFE-LARKIN COMPOSITION RULE FROM THE CONSTRAINT

We can recover simply the IL composition rules by applying the constraint $n_f + n_b = 1$. The external current is associated to the conduction electrons and to the bosons b ,

$$\mathbf{J} = \mathbf{J}_c + \mathbf{J}_b, \quad (\text{D1})$$

but introducing now the fictitious field \mathbf{e} and the external field \mathbf{E} , we get

$$\begin{aligned} \mathbf{J}_c &= \sigma_c \mathbf{E}, \\ \mathbf{J}_b &= \sigma_b (\mathbf{E} + \mathbf{e}), \\ \mathbf{J}_f &= \sigma_f \mathbf{e}. \end{aligned} \quad (\text{D2})$$

We apply $\mathbf{J}_f + \mathbf{J}_b = 0$ to Eq. (D2) and get

$$\mathbf{e} = \frac{-\sigma_b}{\sigma_f + \sigma_b} \mathbf{E}, \quad (\text{D3})$$

which leads to

$$\sigma = \sigma_c + \frac{\sigma_f \sigma_b}{\sigma_f + \sigma_b}. \quad (\text{D4})$$

APPENDIX E: EVALUATION OF THE POLARIZATION AND SELF-ENERGY OF THE BOSONS AT THE QUANTUM CRITICAL POINT

1. Self-energy

$$\Sigma_b(\Omega_n) = \text{bubble diagram with } a_\mu \text{ and } b \text{ lines};$$

This self-energy captures the effect of the gauge fields on the boson propagator. This effect is subdominant in all regimes but in regimes I where, because of the gap in the particle-hole continuum, the only source of damping for the bosons are the gauge fields. We evaluate Σ_b in regime I where $T \leq E^*$ and the particle-hole continuum is gapped. Renaming $c \rightarrow N\pi/(2m_f v_f)$ and $a \rightarrow 1/(2m_f k_F^2)$, we have

$$\Sigma_b(\Omega_n) = T \sum_n \int \frac{d^d q}{(2\pi)^d} \frac{q^2}{2dm_b^2} \frac{1}{-i\omega_n + aq^2} \frac{1}{c|\omega_n + \Omega_n|/q + aq^2}. \quad (\text{E1})$$

Performing the analytical continuation and integrating over the two branch cuts $\omega_n = 0$ and $\omega_n + \Omega_n = 0$, we get for $\Omega_n \geq 0$,

$$\begin{aligned} &= \int \frac{d\omega}{4i\pi} \coth\left(\frac{\omega}{2T}\right) \frac{d^d q}{(2\pi)^d} \frac{q^2}{2dm_b^2} \left\{ \frac{1}{(-\omega + aq^2 - i\delta)} \frac{1}{[c(-i\omega + \Omega_n)/q + aq^2]} - \frac{1}{(-\omega + aq^2 + i\delta)} \frac{1}{[c(i\omega - \Omega_n)/q + aq^2]} \right\}, \\ &= \int \frac{d\omega}{4i\pi} \coth\left(\frac{\omega}{2T}\right) \frac{d^d q}{(2\pi)^d} \frac{q^2}{2dm_b^2} (i\pi) \delta(-\omega + aq^2) \frac{2aq^2}{a^2 q^4 - (ic\omega/q - c\Omega_n/q)^2} \simeq \frac{-1}{2} \int \frac{d^d q}{(2\pi)^d} \frac{q^2}{2dm_b^2} \coth\left(\frac{aq^2}{2T}\right) \frac{2aq^2}{(icaq - c\Omega_n/q)^2}. \end{aligned}$$

Since this integral is dominated by large q , we get

$$\begin{aligned} \Sigma_b(\Omega_n) &\simeq \frac{1}{2} |\Omega_n|^{(d+2)/2} \int_{\sqrt{2T}}^\Lambda \frac{d^d x}{(2\pi)^d} \frac{a}{4dm_b^2} \frac{x^6}{(ix^2 - 1)^2} \\ &= (A + iB) |\Omega_n|^{(d+2)/2}, \\ A &= \text{Re} \left[\int_0^\Lambda \frac{d^d x}{(2\pi)^d} \frac{a}{4dm_b^2} \frac{x^6}{(ix^2 - 1)^2} \right], \\ B &= \text{Im} \left[\int_0^\Lambda \frac{d^d x}{(2\pi)^d} \frac{a}{4dm_b^2} \frac{x^6}{(ix^2 - 1)^2} \right], \end{aligned} \quad (\text{E2})$$

in the limit where $T \rightarrow 0$. We use in Appendix F the short-hand notation,

$$\Sigma_b(\Omega_n) = f_0^\alpha |\Omega_n|^\alpha, \quad \begin{aligned} \alpha &= (d+2)/2, \\ f_0^\alpha &= A + iB \end{aligned} \quad (\text{E3})$$

2. Polarization

In the following, we evaluate the polarization bubble of the bosons in the three possible regimes at the QCP.

$$\text{bubble diagram with } b \text{ lines and } \mathbf{A}_\mu, \mathbf{A}_\nu \text{ vertices} = \Pi_b(q, i\Omega_n)$$

The generic form of the bosonic polarization is

$$\begin{aligned} \Pi_b(Q, i\Omega_n) &= T \sum_{\omega_n} \int \frac{d^d q}{(2\pi)^d} \frac{q^2 v_b^2}{d} D_b(q, i\omega_n) D_b(q + Q, i\omega_n \\ &\quad + i\Omega_n), \end{aligned} \quad (\text{E4})$$

with v_b the vertex defined in Eq. (36).

3. $T=0$: Form used in the gauge propagator

We evaluate here the bosonic polarization contributing the gauge fields propagator. Here, $v_b = 1/m_b$. At $T=0$, only

undamped holons contribute to the damping of the polarization,

$$\Pi_b(Q, i\Omega_n) = \int d\omega \int \frac{d^d q}{(2\pi)^d} \frac{q^2}{2dm_b^2} \times \frac{1}{-i\omega + aq^2} \frac{1}{-(i\omega + i\Omega_n) + aq^2 + qQ \cos \theta/m_b},$$

with $a=1/(2m_b)$

$$= \frac{2i\pi}{-i} \int \frac{\Omega_{d-1} q^d dq d\cos \theta}{(2\pi)^d} \frac{q^2}{2dm_b^2} \frac{-\Omega_n + iqQ \cos \theta/m_b}{\Omega_n^2 + (qQ \cos \theta/m_b)^2},$$

where Ω_{d-1} is the solid of dimension $d-1$

$$= \int \frac{\Omega_{d-1} q^{d-1} dq}{(2\pi)^{d-1}} \frac{q^2}{2dm_b} \frac{\pi |\Omega_n|}{Q}.$$

4. $T \neq 0$: Form used in transport

a. Regime I: There is a gap between the two Fermi surfaces

The form of the boson propagator is given by Eq. (34) with Π_{fc} given by the frequency dependence of Eq. (19) and Σ_b given by Eq. (E3). We see that the particle-hole contribution Π_{fc} to the polarization is undamped in this regime; the only source of damping Σ_b comes from the gauge fields. For the Kubo formulas, we evaluate the polarization at $q \rightarrow 0$, we need only to retain the damping part of the polarization Σ_b . The boson polarization then writes (with $c=1$ and $a=1/(2m_b)$, $v_b=1/m_b$)

$$\Pi_b(0, i\Omega) = T \sum_n \int \frac{d^d q}{(2\pi)^d} \frac{q^2}{2dm_b^2} \frac{1}{f_0^\alpha |\omega_n|^\alpha + aq^2} \frac{1}{f_0^\alpha |\omega_n + \Omega_n|^\alpha + aq^2}.$$

Considering the two branch cuts at $\omega_n=0$ and $\omega_n+\Omega_n=0$, we get

$$\begin{aligned} &= \int \frac{d\omega}{4i\pi} \coth\left(\frac{\omega}{2T}\right) \frac{d^d q}{(2\pi)^d} \frac{q^2}{2dm_b^2} \left\{ \frac{1}{f_0^\alpha (-i\omega)^\alpha + aq^2} \frac{1}{[f_0^\alpha (-i\omega + \Omega_n)^\alpha + aq^2]} - \frac{1}{f_0^\alpha (i\omega)^\alpha + aq^2} \frac{1}{[f_0^\alpha (-i\omega + \Omega_n)^\alpha + aq^2]} \right. \\ &\quad \left. + \frac{1}{f_0^\alpha (-i\omega)^\alpha + aq^2} \frac{1}{[f_0^\alpha (i\omega + \Omega_n)^\alpha + aq^2]} - \frac{1}{f_0^\alpha (i\omega)^\alpha + aq^2} \frac{1}{[f_0^\alpha (i\omega + \Omega_n)^\alpha + aq^2]} \right\}, \\ &= \int \frac{d\omega}{4i\pi} \coth\left(\frac{\omega}{2T}\right) \frac{d^d q}{(2\pi)^d} \frac{q^2}{2dm_b^2} \left[\frac{1}{f_0^\alpha (-i\omega)^\alpha + aq^2} - \frac{1}{f_0^\alpha (i\omega)^\alpha + aq^2} \right] \left[\frac{1}{f_0^\alpha (-i\omega + \Omega_n)^\alpha + aq^2} + \frac{1}{f_0^\alpha (i\omega + \Omega_n)^\alpha + aq^2} \right]. \end{aligned}$$

We expand the second factor in Ω_n and take the part proportional to $|\Omega_n|$ (since the constant part cancels with the tadpole diagram). We get

$$\begin{aligned} \Pi_b(0, i\Omega_n) &\simeq \int \frac{d\omega}{4i\pi} \coth\left(\frac{\omega}{2T}\right) \frac{d^d q}{(2\pi)^d} \frac{q^2}{2dm_b^2} \alpha |\Omega_n| \frac{2i \sin(\alpha\pi/2) f_0^\alpha \omega^\alpha}{\{[f_0^\alpha \omega^\alpha \cos(\alpha\pi/2) + aq^2]^2 + [\sin(\alpha\pi/2) f_0^\alpha \omega^\alpha]^2\}^{3/2}} \{-2\omega^{\alpha-1} \cos[(\alpha-1)\pi/2] \\ &\quad \times \{[f_0^\alpha \omega^\alpha \cos(\alpha\pi/2) + aq^2]^2 - [\sin(\alpha\pi/2) f_0^\alpha \omega^\alpha]^2\} - 2i\omega^{\alpha-1} \sin[(\alpha-1)\pi/2] [-i \sin(\alpha\pi/2) f_0^\alpha \omega^\alpha] [f_0^\alpha \omega^\alpha \cos(\alpha\pi/2) \\ &\quad + aq^2]\}. \end{aligned} \quad (E5)$$

From the above formulas and using $\alpha=(d+2)/2$, we extract τ_b in all dimensions to get

$$\tau_b \sim -\log T \text{ in } D=2,$$

$$\tau_b \sim T^{5/4} \text{ in } D=3. \quad (E6)$$

b. Regime I': The two Fermi surfaces intersect each other

We start now from Eq. (24) (where we have renamed $\rho_0 c / (\alpha' v_F q_0) \rightarrow c$ and $\rho_0 a \rightarrow a$, $v_b=1/m_b$). We take $\Omega_n \geq 0$,

$$\Pi_b(0, i\Omega_n) = T \sum_n \int \frac{d^d q}{(2\pi)^d} \frac{q^2}{2dm_b^2} \frac{1}{c|\omega_n| + aq^2} \frac{1}{c|\omega_n + \Omega_n| + aq^2},$$

considering the two branch cuts at $\omega_n=0$ and $\omega_n+\Omega_n=0$, we have

$$\begin{aligned}
&= \int \frac{d\omega}{4i\pi} \coth\left(\frac{\omega}{2T}\right) \frac{d^d q}{(2\pi)^d} \frac{q^2}{2dm_b^2} \left\{ \frac{1}{(-ci\omega + aq^2)} \frac{1}{[-c(i\omega - \Omega_n) + aq^2]} - \frac{1}{(ci\omega + aq^2)} \frac{1}{[-c(i\omega - \Omega_n) + aq^2]} \right. \\
&\quad \left. + \frac{1}{(-ci\omega + aq^2)} \frac{1}{[c(i\omega + \Omega_n) + aq^2]} - \frac{1}{(ci\omega + aq^2)} \frac{1}{[c(i\omega + \Omega_n) + aq^2]} \right\}, \\
&= \int \frac{d\omega}{4i\pi} \coth\left(\frac{\omega}{2T}\right) \frac{d^d q}{(2\pi)^d} \frac{q^2}{2dm_b^2} \frac{2ic\omega}{c^2\omega^2 + a^2q^4} \frac{2c\Omega_n + aq^2}{c^2\omega^2 + (c\Omega_n + aq^2)^2}.
\end{aligned}$$

Since the bosonic mass cancels out with the tadpole diagram [see Appendix F or Eq. (G14)], we have to extract the part proportional to Ω_n to get

$$\cong \int \frac{d\omega}{\pi} \coth\left(\frac{\omega}{2T}\right) \frac{d^d q}{(2\pi)^d} \frac{q^2}{2dm_b^2} \frac{c^2\omega\Omega_n}{(c^2\omega^2 + a^2q^4)^2}.$$

From the above formulas, we extract τ_b in all dimensions to get

$$\begin{aligned}
\tau_b &\sim -\log T \text{ in } D=2, \\
\tau_b &\sim T^{1/2} \text{ in } D=3.
\end{aligned} \tag{E7}$$

c. Regime II: Both cases

In this regime, we start with Eq. (22) for the boson propagator, showing $z=3$ (with the renaming $\rho_0/(a'v_F)c \rightarrow c$ and $\rho_0 a \rightarrow a$). We take as well $\Omega_n \geq 0$. Here, v_b is a both more complete since we have to expand $|\omega_n|/(|q+a|)$ in the first order in the vector field a to find v_b . We get

$$v_b = 1/m_b - c\omega_n/q^3. \tag{E8}$$

Since in the integral below

$$\begin{aligned}
&\Pi_b(0, i\Omega_n) \\
&= T \sum_n \int \frac{d^d q}{(2\pi)^d} \frac{q^2 v_b^2}{2d} \frac{1}{c|\omega_n|/q + aq^2} \frac{1}{c|\omega_n + \Omega_n|/q + aq^2},
\end{aligned}$$

considering the two branch cuts at $\omega_n=0$ and $\omega_n+\Omega_n=0$,

$$\begin{aligned}
&= \int \frac{d\omega}{4i\pi} \coth\left(\frac{\omega}{2T}\right) \frac{d^d q}{(2\pi)^d} \frac{q^2 v_b^2}{2d} \left\{ \frac{1}{(-ci\omega/q + aq^2)} \frac{1}{[-c(i\omega - \Omega_n)/q + aq^2]} - \frac{1}{(ci\omega/q + aq^2)} \frac{1}{[-c(i\omega - \Omega_n)/q + aq^2]} \right. \\
&\quad \left. + \frac{1}{(-ci\omega/q + aq^2)} \frac{1}{(c(i\omega + \Omega_n)/q + aq^2)} - \frac{1}{(ci\omega/q + aq^2)} \frac{1}{[c(i\omega + \Omega_n)/q + aq^2]} \right\}, \\
&= \int \frac{d\omega}{4i\pi} \coth\left(\frac{\omega}{2T}\right) \frac{d^d q}{(2\pi)^d} \frac{q^2 v_b^2}{2d} \frac{2ci\omega/q}{(c/q)^2\omega^2 + a^2q^4} \frac{2c\Omega_n/q + aq^2}{(c/q)^2\omega^2 + (c\Omega_n/q + aq^2)^2},
\end{aligned}$$

and taking the part proportional to Ω_n , we get

$$\cong \int \frac{d\omega}{\pi} \coth\left(\frac{\omega}{2T}\right) \frac{d^d q}{(2\pi)^d} \frac{q^2 v_b^2}{2d} \frac{(c/q)^2\omega\Omega_n}{[(c/q)^2\omega^2 + a^2q^4]^2}.$$

From the above formulas, we extract τ_b in all dimensions to get

$$\begin{aligned}
\tau_b &\sim -\log T \text{ in } D=2, \\
\tau_b &\sim T^{1/3} \text{ in } D=3.
\end{aligned} \tag{E9}$$

APPENDIX F: WARD IDENTITIES

In this section, we derive the WI associated to the gauge invariance of our theory. When it is not mentioned, the field

σ has been set to zero at the QCP. The first point of interest is to show that the mass of the gauge fields is zero in the Coulomb phase. The second point is to show that it is non-zero in the Higgs phase. In the case of a purely bosonic gauge theory, this second point is simple and can be found, for example, in the Peshkin–Schroder.⁵² In the case of gauge theory with nonrelativistic fermions, the point is more subtle since the gauge fields a_μ and a_ν are not only coupled to the Higgs boson. Gorkov⁶⁵ was the first to show that the mass is generated in the Higgs phase in the case of a superconductor. Here, we follow Zinn-Justin on page 432,⁶⁴ with a field theoretic derivation of the same result. The possibility of massless Higgs phase, although nongeneric, will appear at the end.

We start from Eq. (27) with the gauge fields both coupled to the spinons f and holons b . For simplicity, we have set

$\sigma=0$ everywhere since this parameter is irrelevant at the QCP,

$$S_0 = - \int d^d x d\tau \sum_{\sigma} f_{\sigma}^{\dagger}(x) \left(\partial\tau + \frac{(\nabla - ie\mathbf{a}/c)^2}{2m_f} + \lambda + E_0 \right) f_{\sigma}(x) \\ + b^{\dagger}(x) \left(\partial\tau + \frac{(\nabla - ie\mathbf{a}/c)^2}{2m_b} + \lambda \right) b(x) \\ + \int d^d x d\tau (b(x) f^{\dagger}(x) c(x) + \text{H.c.}) + H_c. \quad (\text{F1})$$

For each field, we introduce a source term, such as

$$a_{\mu} \rightarrow J_{\mu}, \\ f \rightarrow \bar{\eta}, \\ f^{\dagger} \rightarrow \eta, \\ b \rightarrow \bar{J}_b, \\ b^{\dagger} \rightarrow J_b, \quad (\text{F2})$$

so that

$$S = S_0 + S_{\text{source}}, \quad (\text{F3})$$

with

$$S_{\text{source}} = - \int d^d x d\tau (a_{\mu} J_{\mu} + f^{\dagger} \eta + \bar{\eta} f + \bar{J}_b b + b^{\dagger} J_b).$$

The part of the action S_0 [Eq. (F1)] is invariant under the gauge transformation [Eq. (26)]. Only the source terms S_{source} are affected by the gauge transformation. Using the linearized form of the U(1) algebra, $e^{i\theta} = 1 - i\theta$, we get for the variation of the source term c ,

$$\delta S_{\text{source}} = - \int d^d x d\tau \left(\frac{J_{\mu}}{e} \frac{\partial\theta}{\partial x_{\mu}} + i\theta(\bar{\eta}f - f^{\dagger}\eta) + i\theta(b\bar{J}_b - b^{\dagger}J_b) \right).$$

Now from the change in variables,

$$f \rightarrow f(1 + i\theta), \\ b \rightarrow b(1 - i\theta),$$

$$a_{\mu} \rightarrow a_{\mu} + \frac{\partial\theta}{e \partial x_{\mu}}, \quad (\text{F4})$$

we check that the whole action $S = S_0 + S_{\text{source}}$ is invariant under the U(1) gauge transformation. Hence, $\delta S_{\text{source}} = 0$. Integrating by parts the first term in Eq. (F4), one gets one version of the WI,

$$- \partial_{\mu} J_{\mu} + ie(\bar{\eta}f - f^{\dagger}\eta) + ie(\bar{J}_b b - b^{\dagger}J_b)(\dot{}) = 0. \quad (\text{F5})$$

Equation (F5) is applied to any generating functional for correlation functions. We can first use the generating functional of the source currents $W(J, \eta)$.

$$- \partial_{\mu} J_{\mu} + ie \left(\bar{\eta} \frac{\partial W}{\partial \bar{\eta}} - \frac{\partial W}{\partial \eta} \eta \right) + ie \left(\frac{\partial W}{\partial \bar{J}_b} \bar{J}_b - J_b \frac{\partial W}{\partial J_b} \right) = 0. \quad (\text{F6})$$

However, we can also use the generating functional for the vertices Γ , where Γ is a p -leg vertex, which leads to the more useful WI,

$$- \partial_{\mu} \frac{\partial \Gamma}{\partial a_{\mu}} + ie \left(\frac{\partial \Gamma}{\partial f} f - f^{\dagger} \frac{\partial \Gamma}{\partial f^{\dagger}} \right) + ie \left(b \frac{\partial \Gamma}{\partial b} - \frac{\partial \Gamma}{\partial b^{\dagger}} b^{\dagger} \right) = 0. \quad (\text{F7})$$

To get a better idea, let us derive the WI for the two-leg vertex, which is nothing but the total polarization $\Pi_{\mu\nu}$. We differentiate Eq. (F7) with respect to $a_{\nu}(y)$ to get

$$- \partial_{\mu} \frac{\partial^2 \Gamma}{\partial a_{\nu}(y) \partial a_{\mu}(x)} + ie \left(\frac{\partial^2 \Gamma}{\partial a_{\nu}(y) \partial f(x)} f(x) - f^{\dagger}(x) \frac{\partial^2 \Gamma}{\partial a_{\nu}(y) \partial f^{\dagger}(x)} \right) + ie \left(\frac{\partial^2 \Gamma}{\partial a_{\nu}(y) \partial b(x)} b(x) - b^{\dagger}(x) \frac{\partial^2 \Gamma}{\partial a_{\nu}(y) \partial b^{\dagger}(x)} \right) = 0. \quad (\text{F8})$$

To get the proper vertices, we Fourier transform and then set the sources to zero. We note here that it is possible to set the sources to zero in the Coulomb phase, but not in the Higgs phase where the boson acquires a nonzero mean-field value. There are two cases of interest: (i) the Coulomb phase and (ii) the Higgs phase. We get (i) in the Coulomb phase,

$$- iq^{\mu} \Gamma_{\mu\nu}^2(q, -q) = 0, \quad (\text{F9})$$

which is rewritten, with the notations of the body of this paper, as

$$- iq^{\mu} \Pi_{\mu\nu}(q, -q) = 0. \quad (\text{F10})$$

From Eq. (F10), we see that, in the Coulomb phase, the WI ensures that the mass of the transverse gauge field propagator is zero to all orders. Note that identity (F10) constraints only the mass of the vector fields; since the mass is taken at $q^0 = \omega = 0$, for which the scalar field a_0 is dropping out of Eq. (F10). Now, (ii) in the Higgs phase, the WI writes

$$- iq^{\mu} \Gamma_{\mu\nu}^2(q, -q) + ie \langle b \rangle [\Gamma_{b\nu}^2(q, -q) - \Gamma_{b^{\dagger}\nu}^2(q, -q)] = 0. \quad (\text{F11})$$

We see that the gauge field propagator gets massive as soon as $\Gamma_{b\nu}^2(q, -q) - \Gamma_{b^{\dagger}\nu}^2(q, -q) \neq 0$. This phenomenon is nothing but the Meissner effect for superconductors. Note that it can happen that for special forms of the Fermi surface, $\Gamma_{b\nu}^2(q, -q) - \Gamma_{b^{\dagger}\nu}^2(q, -q) = 0$. We then get the equivalent of massless superconductivity for a U(1) gauge theory.

We can also derive the same kind of WI for the three-leg vertex. Let us take, for example,

$$\Gamma_{a_{\mu} f_{k+q}^{\dagger} f_k} = a_{\mu}(q) \begin{array}{c} \text{---} f_k \\ \text{---} \text{---} \\ \text{---} f_{k+q}^{\dagger} \end{array}$$

We differentiate Eq. (F7) with respect to $f(y)$ and then to $f^\dagger(z)$ and set the source terms to zero, except in the Higgs phase,

$$\begin{aligned} & -\partial_\mu \frac{\partial^3 \Gamma}{\partial a_\mu(x) \partial f^\dagger(z) \partial f(y)} + ie \left(-\frac{\partial^2 \Gamma}{\partial f^\dagger(z) \partial f(x)} \delta_{xy} \right. \\ & \quad \left. - \frac{\partial^2 \Gamma}{\partial f(y) \partial f^\dagger(x)} \delta_{xz} \right) + ie \left(b(x) \frac{\partial^3 \Gamma}{\partial f^\dagger(z) \partial f(y) \partial b(x)} \right. \\ & \quad \left. - \frac{\partial^3 \Gamma}{\partial f^\dagger(z) \partial f(y) \partial b^\dagger(x)} b^\dagger(x) \right) = 0. \end{aligned} \quad (\text{F12})$$

(i) In the Coulomb phase,

$$-iq^\mu \Gamma_{a_\mu^\dagger k+q f_k}^3 + ie[G_f^{-1}(k+q) - G_f^{-1}(k)] = 0. \quad (\text{F13})$$

(ii) In the Higgs phase, it comes

$$\begin{aligned} & -iq^\mu \Gamma_{a_\mu^\dagger k+q f_k}^3 + ie[G_f^{-1}(k+q) - G_f^{-1}(k)] + ie\langle b \rangle \\ & \quad \times \left(\frac{\partial^3 \Gamma}{\partial b_q \partial f_{k+q}^\dagger \partial f_k} - \frac{\partial^3 \Gamma}{\partial b_q^\dagger \partial f_k^\dagger \partial f_{k+q}} \right) = 0. \end{aligned}$$

Quite generically, the p -leg vertex is related to the $(p-1)$ -leg vertex through the WI. Note that a relation similar to Eq. (F13) can be established for the ferromagnetic QCP using the translational invariance instead of the gauge invariance; one can follow the same steps using the Noether theorem associated with translation invariance, instead of the equivalent of it, associated with U(1) local invariance, which we derived here.

APPENDIX G: DIRECT CHECK OF THE VANISHING OF THE MASSES

In this section, we directly check that the masses of the gauge field propagator vanish in the Coulomb phase at the first order in perturbation theory.

1. Fermion part

Let us start with the fermions and check the following cancellation:

$$\Pi_f(0,0) = \begin{array}{c} f \\ \nearrow \quad \searrow \\ \text{---} \quad \text{---} \\ \searrow \quad \nearrow \\ f \end{array} + \begin{array}{c} \text{---} \\ \nearrow \quad \searrow \\ \text{---} \end{array} = 0$$

$$\begin{aligned} \Pi_f(0,0) &= \delta_{ij} \frac{T}{2m_f^2 \omega_n} \sum \int \frac{d^d k}{(2\pi)^d} \frac{k^2}{d} \frac{1}{(i\omega_n - \epsilon_k^0)^2} \\ &+ \frac{T}{2m_f \omega_n} \sum \int \frac{d^d k}{(2\pi)^d} \frac{1}{(i\omega_n - \epsilon_k^0)}, \end{aligned}$$

with $\epsilon_k^0 = k^2/(2m_f) + \epsilon_f$. Relating the first term to the second through the identity

$$(-2m_f^2) \frac{\partial}{\partial m_f} \frac{1}{(i\omega_n - \epsilon_k^0)} = \frac{k^2}{(i\omega_n - \epsilon_k^0)},$$

we get

$$\Pi_f(0,0) = \left(-\frac{1}{d} \frac{\partial}{\partial m_f} + \frac{1}{2m_f} \right) \int \frac{d^d k}{(2\pi)^d} n_F(\epsilon_k^0). \quad (\text{G1})$$

Noticing that

$$\int \frac{d^d k}{(2\pi)^d} n_F(\epsilon_k^0) = \rho_f \sim m_f^{d/2},$$

we finally get at the first order in perturbation theory

$$\Pi_f(0,0) = 0. \quad (\text{G2})$$

2. Holon part

The bosonic part follows the same steps as the fermionic one,

$$\Pi_b(0,0) = \begin{array}{c} b \\ \nearrow \quad \searrow \\ \text{---} \quad \text{---} \\ \searrow \quad \nearrow \\ b \end{array} + \begin{array}{c} \text{---} \\ \nearrow \quad \searrow \\ \text{---} \end{array} = 0$$

$$\begin{aligned} \Pi_b(0,0) &= \delta_{ij} \frac{T}{2m_b^2 \omega_n} \sum \int \frac{d^d q}{(2\pi)^d} \frac{q^2}{d} \frac{1}{[i\omega_n - q^2/(2m_b)]^2} \\ &+ \frac{T}{2m_b \omega_n} \sum \int \frac{d^d q}{(2\pi)^d} \frac{1}{[i\omega_n - q^2/(2m_b)]}. \end{aligned}$$

Relating the first term to the second term through the identity

$$(-2m_b^2) \frac{\partial}{\partial m_b} \frac{1}{[i\omega_n - q^2/(2m_b)]} = \frac{q^2}{[i\omega_n - q^2/(2m_b)]},$$

we get

$$\Pi_b(0,0) = \left(-\frac{1}{d} \frac{\partial}{\partial m_b} + \frac{1}{2m_b} \right) \int \frac{d^d q}{(2\pi)^d} n_B[q^2/(2m_b)].$$

$$\int \frac{d^d q}{(2\pi)^d} n_B[q^2/(2m_b)] = \Omega_d \frac{m_b^{d/2}}{(2\pi)^d} \int x^{d-1} dx n_B(x^2),$$

with Ω_d as the solid angle in d dimensions, we finally get at the first order in perturbation theory,

$$\Pi_b(0,0) = 0. \quad (\text{G3})$$

APPENDIX H: CONDUCTION ELECTRON'S LIFETIME

In this appendix, we give the evaluation of the temperature dependence of the imaginary part of $\text{Im} \Sigma_c$. We work in $D=3$ and

$$\Sigma_c(T) = gT \sum_n \int \frac{d^d q}{(2\pi)^d} \frac{q}{c|\omega_n - \pi T| + aq^3} \frac{1}{i\omega_n - \epsilon_{k+q}^0}, \quad (\text{H1})$$

where the frequency $\omega_n = (2n+1)\pi T$. We close the contour around the two branch cuts for $\omega_n=0$ and $\omega_n - \pi T=0$ to get

$$\begin{aligned} \Sigma_c(T) &= -g \int \frac{d\omega}{4i\pi} \coth\left(\frac{\omega}{2T}\right) \int \frac{qd^d q}{(2\pi)^d} \\ &\quad \times \left[\frac{1}{-i\omega + aq^3} \frac{1}{\omega + i\pi T - \alpha v_F q_x} \right. \\ &\quad \left. - \frac{1}{i\omega + aq^3} \frac{1}{\omega + i\pi T - \alpha v_F q_x} \right] \\ &= -g \int \frac{d\omega}{4i\pi} \tanh\left(\frac{\omega}{2T}\right) \int \frac{qd^d q}{(2\pi)^d} \\ &\quad \times \left[\frac{1}{i\omega + c\pi T + aq^3} \frac{1}{\omega + i\delta - \alpha v_F q_x} \right. \\ &\quad \left. - \frac{1}{i\omega + c\pi T + aq^3} \frac{1}{\omega - i\delta - \alpha v_F q_x} \right], \\ &= -g \int \frac{d\omega}{4i\pi} \coth\left(\frac{\omega}{2T}\right) \int \frac{qd^d q}{(2\pi)^d} \\ &\quad \times \left[\frac{2i\omega}{c^2\omega^2 + a^2q^6} \frac{1}{\omega + i\pi T - \alpha v_F q_x} \right] \\ &= -g \int \frac{d\omega}{4i\pi} \tanh\left(\frac{\omega}{2T}\right) \int \frac{qd^d q}{(2\pi)^d} \\ &\quad \times \left[\frac{2}{i\omega + c\pi T + aq^3} \frac{1}{\omega + i\delta - \alpha v_F q_x} \right], \end{aligned}$$

Taking the integration over q_x leads to

$$\begin{aligned} \Sigma_c(T) &= \frac{g}{\alpha v_F} \int \frac{d\omega}{4\pi} \coth\left(\frac{\omega}{2T}\right) \int \frac{\Omega_d q^{d-1} dq}{(2\pi)^{d-1}} \frac{ic\omega}{c^2\omega^2 + a^2q^6} \\ &\quad + \frac{g}{\alpha v_F} \int \frac{d\omega}{4\pi} \tanh\left(\frac{\omega}{2T}\right) \int \frac{\Omega_d q^{d-1} dq}{(2\pi)^{d-1}} \frac{1}{i\omega + c\pi T + aq^3}, \end{aligned}$$

where Ω_d is the solid angle of dimension d . This integral is dominated by the low energy part of the first term (the high

energy part of the first and second terms cancels out) which leads to

$$\text{Im } \Sigma_c(T) = \frac{g}{\alpha v_F} \int_{a_{\text{IR}}}^T \frac{d\omega}{2\pi} \frac{T}{\omega} \int \frac{\Omega_d q^{d-1} dq}{(2\pi)^{d-1}} \frac{c\omega}{c^2\omega^2 + a^2q^6},$$

where a_{IR} is a IR cutoff. Taking $d=3$ and changing variables for $x=q^3/\omega$, we get

$$\begin{aligned} \text{Im } \Sigma_c(T) &= \frac{g}{\alpha v_F c} \int_{a_{\text{IR}}}^T d\omega \frac{T}{\omega} \int_0^\infty \frac{4\pi dx}{3(2\pi)^3} \frac{1}{1+a^2x^2}, \\ &\simeq T \log\left(\frac{T}{a_{\text{IR}}}\right). \quad (\text{H2}) \end{aligned}$$

The question is now to determine the cutoff a_{IR} . Since we work at finite temperature, there are two sources of IR cut off which are E^* and $m_b(T)$, with $m_b(T)$ is the temperature dependence of the holon mass,

$$a_{\text{IR}} = \max[E^*, m_b(T)].$$

Here, $m_b(T)$ is determined by evaluating the corrections to scaling

where g_4 is the coupling constant associated to the ϕ^4 -holon field theory, if it is there. One can check that the first diagram goes like $T^{(d+z-2)/z}$, the second one like $T^{(d+2)/2}$, and the third one like $T^{5/3}$ in $D=3$. Hence, in $D=3$,

$$m_b(T) \simeq T^{4/3}.$$

Note that the lines are full and that we must use the Eliashberg theory for this check. Hence, in this model, in the intermediate energy regime, $m_b(T) \ll E^*$. We get

$$\text{Im } \Sigma_c(T) \simeq T \log\left(\frac{T}{E^*}\right). \quad (\text{H3})$$

¹For some compounds such as CeCoIn₅, the field excited level is found at quite low temperatures, less than 100 K, and the assumption of a well formed Kramers doublet can be questioned.

²G. Stewart, Rev. Mod. Phys. **56**, 755 (1984); **73**, 797 (2001).

³P. Coleman, C. Pépin, Q. Si, and R. Ramazashvili, J. Phys.: Condens. Matter **13**, R723 (2001).

⁴H. v. Löhneysen, A. Rosch, M. Vojta, and P. Wolfe, Rev. Mod. Phys. **79**, 1015 (2007).

⁵P. Gegenwart, Q. Si, and F. Steglich, arXiv:0712.2045 Nat. Phys. (to be published).

⁶By comparison, the notorious linear resistivity in high temperature superconductors holds only for a bit more than one decade of energy.

⁷M. Neumann *et al.*, Science **317**, 1356 (2007).

⁸M. A. Ruderman and C. Kittel, Phys. Rev. **96**, 99 (1954).

⁹A. Auerbach and K. Levin, Phys. Rev. Lett. **57**, 877 (1986); A. Auerbach and K. Levin, Phys. Rev. B **34**, 3524 (1986).

- ¹⁰A. J. Millis and P. A. Lee, Phys. Rev. B **35**, 3394 (1987).
- ¹¹F. Steglich, J. Aarts, C. D. Bredl, W. Lieke, D. Meschede, W. Franz, and H. Schafer, Phys. Rev. Lett. **43**, 1892 (1979).
- ¹²S. Doniach, Physica B & C **91**, 231 (1977).
- ¹³C. Lacroix and M. Cyrot, Phys. Rev. B **20**, 1969 (1979).
- ¹⁴J. A. Hertz, Phys. Rev. B **14**, 1165 (1976).
- ¹⁵A. J. Millis, Phys. Rev. B **48**, 7183 (1993).
- ¹⁶T. Moriya and T. Takimoto, J. Phys. Soc. Jpn. **64**, 960 (1995).
- ¹⁷Ar. Abanov, A. V. Chubukov, and J. Schmalian, Adv. Phys. **52**, 119 (2003).
- ¹⁸J. Rech, C. Pépin, and A. V. Chubukov, Phys. Rev. B **74**, 195126 (2006).
- ¹⁹A. Rosch, A. Schroder, O. Stockert, and H. v. Lohneysen, Phys. Rev. Lett. **79**, 159 (1997); A. Rosch, *ibid.* **82**, 4280 (1999).
- ²⁰N. J. Curro, B. L. Young, J. Schmalian, and D. Pines, Phys. Rev. B **70**, 235117 (2004).
- ²¹Q. Si *et al.*, Nature (London) **413**, 804 (2001); D. R. Grempel and Q. Si, Phys. Rev. Lett. **91**, 026401 (2003).
- ²²S. Pankov, S. Florens, A. Georges, G. Kotliar, and S. Sachdev, Phys. Rev. B **69**, 054426 (2004).
- ²³T. Senthil, S. Sachdev, and M. Vojta, Phys. Rev. Lett. **90**, 216403 (2003); T. Senthil, M. Vojta, and S. Sachdev, Phys. Rev. B **69**, 035111 (2004).
- ²⁴P. Coleman, J. B. Marston, and A. J. Schofield, Phys. Rev. B **72**, 245111 (2005).
- ²⁵M. Roger, Phys. Rev. Lett. **64**, 297 (1990).
- ²⁶G. Misguich, B. Bernu, C. Lhuillier, and C. Waldtmann, Phys. Rev. Lett. **81**, 1098 (1998).
- ²⁷I. Paul, C. Pépin, and M. R. Norman, Phys. Rev. Lett. **98**, 026402 (2007).
- ²⁸C. Pépin, Phys. Rev. Lett. **98**, 206401 (2007).
- ²⁹S. Burdin, D. R. Grempel, and A. Georges, Phys. Rev. B **66**, 045111 (2002).
- ³⁰At low energies, Senthil *et al.* (Ref. 23) find a bosonic contribution to the conductivity which varies like $-1/\log T$. This contribution is actually a correction to the conduction electron's residual resistivity ρ_0 . Hence, $-\log T \ll \rho_0^{-1}$ and the range of validity in temperature is exponentially small: $T \ll \exp(-1/\rho_0) \ll 1$. The contribution $-1/\log T$ they talk about is thus completely undetectable experimentally; this regime is dominated by the residual resistivity of the conduction electrons. A second comment is that the lifetime of the bosons [Eq. (E2)] differs from the one found in Ref. 23; we find their exponent in $D=2$ but not in $D=3$.
- ³¹A. Benlagra and C. Pépin, Phys. Rev. Lett. **100**, 176401 (2008).
- ³²P. Fulde and R. A. Ferrel, Phys. Rev. **135**, A550 (1964); A. I. Larkin and Y. Ovchinnikov, Sov. Phys. JETP **20**, 762 (1965).
- ³³T. M. Rice, Phys. Rev. B **2**, 3619 (1970).
- ³⁴M. Ferrero, F. Becca, M. Fabrizio, and M. Capone, Phys. Rev. B **72**, 205126 (2005).
- ³⁵C. Knecht, N. Blumer, and P. G. J. van Dongen, Phys. Rev. B **72**, 081103(R) (2005).
- ³⁶J. Bünemann *et al.*, J. Phys.: Condens. Matter **19**, 436206 (2007).
- ³⁷S. Biermann, L. de' Medici, and A. Georges, Phys. Rev. Lett. **95**, 206401 (2005).
- ³⁸L. De Leo, M. Civelli, and G. Kotliar, arXiv:cond-mat/0702559 (unpublished).
- ³⁹P. Sun and G. Kotliar, Phys. Rev. Lett. **91**, 037209 (2003).
- ⁴⁰L. de' Medici, A. Georges, G. Kotliar, and S. Biermann, Phys. Rev. Lett. **95**, 066402 (2005).
- ⁴¹A. Filippetti and V. Fiorentini, Phys. Rev. Lett. **98**, 196403 (2007).
- ⁴²P. A. Lee, N. Nagaosa, and X.-G. Wen, Rev. Mod. Phys. **78**, 17 (2006).
- ⁴³P. W. Anderson, Science **235**, 1196 (1987).
- ⁴⁴J. Marston and I. Affleck, Phys. Rev. B **39**, 11538 (1989).
- ⁴⁵P. A. Lee and N. Nagaosa, Phys. Rev. B **46**, 5621 (1992).
- ⁴⁶T. C. Hsu, Phys. Rev. B **41**, 11379 (1990).
- ⁴⁷P. Coleman, Phys. Rev. B **29**, 3035 (1984).
- ⁴⁸P. W. Anderson, Science **235**, 1196 (1987).
- ⁴⁹P. Nozières, Ann. Phys. (Paris) **10**, 19 (1985).
- ⁵⁰The reader might wonder why the coefficient of q^2 is not multiplied by N . The reason is that we can *a priori* decide to maintain the number of particles constant when going from $N=2$ to large N . Hence, the Fermi wave vector is rescaled like $k_F \rightarrow 2k_F/N$. The coefficient of q^2 comes from the UV sector of the theory and as such acts as an additional coupling constant. This leaves us the latitude to rescale it the way we want.
- ⁵¹B. L. Altshuler, L. B. Ioffe, and A. J. Millis, Phys. Rev. B **50**, 14048 (1994).
- ⁵²M. E. Peskin and D. V. Schroeder, *Quantum Field Theory* (Westview Press/Addison-Wesley, 1995), Chap. 20.
- ⁵³N. Read and D. M. Newns, J. Phys. C **16**, 3273 (1983); N. Read, *ibid.* **18**, 2651 (1985).
- ⁵⁴M. Y. Reizer, Phys. Rev. B **39**, 1602 (1989); M. Y. Reizer, *ibid.* **40**, 11571 (1989).
- ⁵⁵In the artificial case where the dispersion is purely linear, the polarization is massless at $T=0$.
- ⁵⁶D. Belitz, T. R. Kirkpatrick, and T. Vojta, Phys. Rev. B **55**, 9452 (1997).
- ⁵⁷L. B. Ioffe and A. I. Larkin, Phys. Rev. B **39**, 8988 (1989).
- ⁵⁸In order to simplify the discussion, we have neglected the field σ in this section. In all rigor, it should be taken into account.
- ⁵⁹Note that the gauge invariance seems to be broken in the expansion to the first order in the gauge fields. It is not the case since one must expand as well to the first order in $\nabla\theta$ when checking the gauge invariance of the action.
- ⁶⁰G. D. Mahan, *Many-Particle Physics* (Plenum, New York, 2001), p. 696.
- ⁶¹Note that in this formula, the masses are band masses and not thermodynamic masses.
- ⁶²N. Read, J. Phys. C **18**, 2651 (1985).
- ⁶³Ki-Seok Kim, Phys. Rev. B **72**, 035109 (2005).
- ⁶⁴J. Zinn-Justin, *Quantum Field Theory and Critical Phenomena* (Oxford Science, Oxford, 1989).
- ⁶⁵L. P. Gorkov, Sov. Phys. JETP **9**, 1364 (1959).